Research Square

Preprints are preliminary reports that have not undergone peer review.
They should not be considered conclusive, used to inform clinical practice,
or referenced by the media as validated information.

The tumor microbiome is implicated in breast cancer prognosis

Jia Zhu
Department of Breast Surgery, The First Affiliated Hospital of Nanchang University.
Jie Wu
The Second Affiliated Hospital of Nanchang University
Changgan Mo
Hechi Hospital Affiliated to Youjiang Medical University for Nationalities
Siyuan Liang
Fudan University Shanghai Cancer Center
Tao Lian
Department of Breast Surgery,The First Affiliated Hospital of Nanchang University
Tiantian Qi
Department of Breast Surgery,The First Affiliated Hospital of Nanchang University
Rongbin Qiu
Department of Breast Surgery,The First Affiliated Hospital of Nanchang University
Xiaoting Yu
Department of Breast Surgery,The First Affiliated Hospital of Nanchang University
Xiuge Tang
Hechi Hospital Affiliated to Youjiang Medical University for Nationalities
Biao Wu (cdyfyrxk@126.com)
The First Affiliated Hospital of Nanchang University https://orcid.org/0000-0002-5123-9201

Research

Keywords: Breast cancer, Tumor microbiome, Immune microenvironment, Prognosis

Posted Date: October 29th, 2020

DOI: https://doi.org/10.21203/rs.3.rs-97367/v1

License: This work is licensed under a Creative Commons Attribution 4.0 International License.
Read Full License

Abstract

Background: Some breast cancer patients are prone to recurrence and metastasis. Increasing evidence suggests that the breast tissue contains a diverse population of bacteria, which may be modulating the risk of breast cancer development or progression. However, the extent of microbial contribution to the tumor immune microenvironment in breast cancer remains unknown. Here, we explored the potential influence of the tumor microbiota on the local immune microenvironment and breast cancer prognosis.

Methods: Using 16S rRNA gene sequencing, we analyzed the tumor microbiome composition and identified bacteria that were differentially abundant between breast cancer patients with recurrence or metastasis (R/M) and those without recurrence or metastasis (NRM). We performed total RNA sequencing in tumor tissues from patients in both groups to determine differentially expressed genes (DEGs). The landscape of tumor-infiltrating immune cells (TIICs) subtypes in the tumor immune microenvironment was analyzed using CIBERSORT, based on the gene expression profiling of tumor tissues. Differences in the tumor microbiomes were then correlated with DEGs and differences in TIICs, in order to determine how microbial abundance may contribute to cancer progression.

Results: Microbial alpha-diversity was higher in NRM patients than in R/M patients. The composition and functions of the tumor microbiome communities differed between the two groups. We found higher alpha-diversity, higher abundance of *Ruminococcus*, *Butyrivibrio*, and *Deinococcus*, and lower abundance of *Microbacterium* could serve as a predictor of better prognosis in breast cancer patients. We also found that 16 genes, including CD36, showed differential expression in NRM compared to R/M, and differences in the composition of TIICs were observed between the two groups. In addition, we observed that the different tumor microbiome profiles were associated with DEGs and differences in TIICs between the two groups.

Conclusions: The tumor microbiome may affect the prognosis of breast cancer patients by influencing the tumor immune microenvironment. Thus, the tumor microbiome may be a useful prognostic indicator.

Background

Microbes colonize areas that are directly exposed to the air and surroundings, including the mouth, nostrils, skin, stomach, and the gastrointestinal and urogenital tracts [1]. Viral or bacterial infection is the third highest contributor to the development of cancer [2, 3]. It is estimated that 15–20% of malignancies are caused by microbial pathogens, and even more malignancies are related to alterations in microbial communities that colonize human tissues [3–6]. The microbiome is associated with a variety of malignancies, including gastric, colon, liver, lung, and skin cancers and lymphoma. Perhaps the strongest linkages so far have been found between gastric cancer and *Helicobacter pylori*, and between colon cancer and *Fusobacterium* [7–12]. The microbiome may contribute to carcinogenesis by inducing chronic inflammation, altering cellular processes, and triggering uncontrolled innate and adaptive immune responses [12]. Chronic, persistent inflammation increases the risk of cancer [5, 6, 13].

Skin and oral bacteria can access the mammary ducts through the nipple [14–16]. Recent studies suggested that some mammary gland bacteria may be derived from the gut by an endogenous entero-mammary pathway [17–20]. Several studies have reported that commensal microbiota are abundant in breast cancer [21–23]. One study found that the diversity of commensal bacteria in breast cancer tissues was similar to that in other organs (such as the intestine), and higher than that in the vagina [22]. Breast tumors show enrichment in taxa of low abundance in normal tissues, including the genera *Fusobacterium, Atopobium, Gluconacetobacter, Hydrogenophaga*, *and Lactobacillus* [21]. The relative abundance of *Bacillus, Enterobacteriaceae*, and *Staphylococcus* is higher in breast cancer tissues than in normal ones, *Escherichia coli* and *Staphylococcus epidermidis* isolated from breast cancer tissues can induce DNA double-strand breaks in HeLa cells [23]. These results suggest that breast cancer is associated with changes in the breast microbiome, and that the tumor microbiome may play a role in the development and progression of breast cancer.

The breast tissue is composed of epithelial cells, stroma, and a mucosal immune system that together form a complex microenvironment. Myeloid and lymphoid cells are present and localized to lobules, with cytotoxic T and dendritic cells directly integrated into the epithelium [24]. The development of the mucosal immune system is a direct result of microbial exposure, and the presence of immune effectors within the complex microenvironment of the breast is suggestive of a breast microbiome [21]. Immune cell function has also been extensively linked to progression of breast cancer [25–27]. The breast microbiome may affect the development or progression of breast cancer by influencing the tumor immune microenvironment (TIME). However, the extent of the microbial contribution to the TIME remains unknown.

In this study, we sought to explore the influence of tumor microbiome on the local immune microenvironment and on prognosis of patients with breast cancer. We compared the tumor microbiome between breast cancer patients with or without metastasis/recurrence, and we evaluated the relationships among tumor microbial diversity, tumor microbial abundance, and disease-free survival (DFS). Lastly, we explored whether differences between the tumor microbiomes in the two groups of patients correlated with differences in gene expression and fraction of tumor-infiltrating immune cells (TIICs). Our goal was to begin clarifying how the tumor microbiome may contribute to breast cancer progression.

Methods

Study subjects

All patients with breast cancer diagnosed by pathological examination at the First Affiliated Hospital of Nanchang University were retrospectively included in the study. Demographic and clinical data were collected from medical records and telephone interviews; data included age, height, weight, ethnicity, cancer stage, tumor molecular subtype, medical history (e.g. with or without breast fibroma, mammary duct ectasia, intraductal papilloma, mastitis), history of preoperative chemotherapy (e.g. cyclophosphamide, anthracycline, paclitaxel), preoperative use of antibiotics, and disease-free survival

(DFS) time after surgery. The study was approved by the Ethics Committee of the First Affiliated Hospital of Nanchang University, Nanchang, Jiangxi, China and informed consent was obtained from all subjects.

Breast cancer tissues from all the patients were collected during surgery and stored at -80°C. A total of 106 patients were included in the study, after matching with respect to age, stage, and prior therapies (antibiotics and neoadjuvant treatment), 57 patients were divided into two groups: 26 patients with no recurrence or metastasis (≥6-years DFS), hereafter called the NRM group; and 31 patients with recurrence or metastasis (<6-years DFS), hereafter called the R/M group.

16S rRNA gene sequencing

Bacterial DNA from breast cancer tissue was extracted using the E.Z.N.A.® soil DNA Kit (Omega Biotek, Norcross, GA, USA). The V3-V4 regions of bacterial 16S rRNA gene were amplified using the primers 338F (5'-ACTCCTACGGGAGGCAGCAG-3') and 806R (5'-GGACTA CHVGGGTWTCTAAT-3'). The amplicon library was used for paired-end sequenced (2× 300bp) on an Illumina MiSeq platform (Illumina, San Diego, CA, USA).

16S rRNA gene bioinformatics analyses

Amplicon sequence variants (ASVs) were generated after filtering, denoising, merging, and removal of chimeric of raw sequences using the QIIME2 dada2 plugin [28]. The QIIME2 feature-classifier plugin was then used to align ASV sequences to GREENGENES database and annotated [29]. Kruskal-Wallis, Wilcoxon, and Linear discrimination analysis (LDA) effect size (LEfSe) were applied to identify the bacteria differing in abundance between the two groups [30], and the P-value was adjusted using the Bonferroni method. Diversity metrics were calculated using the QIIME2 core-diversity plugin.

The alpha diversity of the microbiome was calculated as observed OTUs and Chao1 index. The beta diversity was assessed using the Bray-Curtis metrics, unweighted UniFrac and weighted UniFrac. Permutational Multivariate Analysis of Variance (PERMANOVA) was used to evaluate the diversity differences between groups, and principal coordinate analyses (PCoA) were performed to visualize the distance between samples [31]. Partial least squares discriminant analysis (PLS-DA) was applied as a supervised model to reveal the microbiota variation between the two groups, using the "plsda" function in R package "mixOmics", and the classification performance between the two groups by PLS-DA based on tumor microbiome markers was assessed using the receiver operator characteristic (ROC) curve [32]. Co-occurrence analysis was performed to calculate Spearman's rank correlations between predominant bacteria. Phylogenetic Investigation of Communities by Reconstruction of Unobserved States (PICRUSt) was applied to predict the potential function of tumor microbiomes [33]. The Dunn test was applied for the predicted functions, and P-values were corrected using the Bonferroni method [34].

RNA sequencing (RNA-Seq)

Total RNA was extracted from tissue samples using TRIzol. The RNA integrity was verified with an Agilent 2100 bioanalyzer (Agilent, Santa Clara, CA, USA). Sequencing libraries were generated using NEBNext®

Ultra™ RNA Library Prep Kit for Illumina® (NEB, MA, USA). RNA libraries were sequenced using the Illumina NovaSeq6000 platform to obtain 150 bp paired-end reads.

RNA-Seq bioinformatic analysis

HISAT2 [35] was used to align reads to the reference genome. The software StringTie was used to map reads in order to estimate the expression of each gene transcript [36].

Gene expression levels were estimated by FPKM [37]. Differential expression analysis between the two groups was performed using DESeq, and adjustment for multiple-testing with the procedure of Benjamini and Hochberg yielded significant differentially expressed genes (DEGs) based on the criteria of log2|fold change| ≥ 1 and adjusted $P < 0.05$ [38, 39]. Gene Ontology (GO) enrichment analysis of DEGs was performed using the clusterProfiler R package [40]. Kyoto Encyclopedia of Genes and Genomes (KEGG) enrichment analysis of DEGs was performed using the clusterProfiler R package [40] and gage R package [41].

Evaluation of infiltrating immune cells in breast cancer tissue

CIBERSORT [42] was used to examine the relative fractions of 22 TIIC types based on the gene expression profiling of tumor tissues; 22 TIIC types included B cells, T cells, natural killer cells, macrophages, and dendritic cells, and others. CIBERSORT has been shown to accurately determine the lanscape of TIICs in tumors of the breast, lung, colon, and prostate [43-45].

Statistical analysis

Demographic and clinical characteristics were compared between the two different groups using Student's *t* test or chi-squared test in SPSS 16.0 (IBM, Chicago, IL, USA). Kaplan-Meier survival curves were used to estimate DFS, and differences between the two patient groups were assessed by log-rank test. Associations of gene expression and TIICs with microbial abundance were assessed using Spearman's rank correlation in R software (version 3.3.2).

Results

Baseline demographic and clinical characteristics of study patients

The demographic and clinical charateristics of the 26 patients in the NRM group and the 31 patients in the R/M group are shown in Table 1. No significant differences were observed in age, body mass index, ethnicity, cancer stage, neoadjuvant chemotherapy, antibiotics use (pre-surgery), or tumor molecular subtypes.

Tumor microbial diversity was significantly different between the two groups and was associated with prognosis

To explore the potential association of the tumor microbiome composition with prognosis of breast cancer patients, we investigated differences in the microbiome composition of tumor tissues between NRM and R/M patients. A total of 2,610,661 raw reads were obtained from all 57 samples, with an average number of reads of 45,801±10,702 per sample (Additional file 1:Table S1). After quality control and removal of noise and chimeras, a total of 2,241,646 high-quality sequences were generated across all samples (Additional file 1:Table S2) and clustered into 4,569 OTUs (Additional file 2:Figure S1; Additional file 1:Table S3). The rarefaction curves approached saturation, suggesting that the majority of OTUs were recovered (Additional file 2:Figure S2).

Richness and evenness were higher in the tumor microbiome of NRM subjects than in that of R/M patients in terms of alpha diversity, as measured in observed OTUs (P=0.024, Wilcoxon rank sum test, Fig. 1a) and Chao1 index (P=0.024, Wilcoxon rank sum test, Fig. 1b). However, the beta diversity was not significantly different between the two groups based on the Bray-Curtis index (P=0.853, Fig. 1c), weighted UniFrac index (P=0.891, Fig. 1d), or unweighted UniFrac index (P=0.591, Fig. 1e) (all P from PERMANOVA). The PCoA plot was not completely separated based on the Bray-Curtis metrics (Fig. 1f), weighted UniFrac (Fig. 1g), or unweighted UniFrac metrics (Fig. 1h).

According to the PLS-DA, the tumor microbiomes of the NRM and R/M groups were clearly differentiated into two independent clusters, suggesting that their composition was significantly different (Fig. 1i). The area under the curve (AUC) was 0.9975, indicating that the prediction model obtained by the PLS-DA analysis is reliable. Thus, the tumor microbiome in R/M patients may be a strong predictor of recurrence or metastasis in breast cancer patients (Fig. 1g).

Based on the alpha diversity results, we tested the relationship between tumor microbial diversity and DFS by stratifying the patients in two groups based on median diversity obtained by observed OTUs index. We found that patients with high alpha diversity showed significantly longer DFS (median survival: 78 months) than those with low alpha diversity (median survival: 30 months) (Fig. 2).

The relationship between tumor microbial diversity and prognosis actually allowed the stratification of breast cancer patients according to whether their alpha diversity was high or low. These findings support the idea that tumor microbial diversity may be a prognostic predictor, and suggest that tumor microbiome composition may influence tumor progression.

Tumor microbiome composition was significantly different between NRM and R/M patients and was associated with prognosis

To identify marked differences in the predominance of bacterial taxa between NRM and R/M patients, different taxonomy levels were compared using LEfSe analysis based on Kruskal-Wallis and Wilcoxon test to detect bacterial taxa with significant differential abundances between NRM and R/M patients. LEfSe then was performed using LDA to estimate the effect size of each differentially abundant taxa with the criteria of LDA > 2 and P < 0.05. The tumors of NRM patients exhibited a predominance of Ruminococcaceae at the family level and *Anaerostipes* at the genus level. In contrast, the tumors of R/M

patients were dominated by Bacilli at the class level, Tissierellaceae and Enterococcaceae at the family level, Lactobacillales at the order level, and *Anaerococcus* and *Dechloromonas* at the genus level (Fig. 3a,b).

The relative abundance of nine genera differed significantly between NRM and R/M. Four genera were enriched in R/M: *Dechloromonas, Anaerococcus, Thiothrix* and *Microbacterium*. Conversely, five genera were less abundant in R/M: *Ruminococcus, Anaerostipes, Weissella, Butyrivibrio* and *Deinococcus* (adjusted $P < 0.05$, Kruskal-Wallis and Wilcoxon; Fig. 4; Additional file 1: Table S4).

We then stratified patients into high or low categories based on their median relative abundance of the four genera *Ruminococcus, Butyrivibrio, Deinococcus,* and *Microbacterium*. Risk of recurrence or metastasis was significantly lower for breast cancer patients with higher abundance of *Ruminococcus* [hazard ratio (HR)=0.4554, 95% confidence interval (CI) 0.2169-0.9560], *Butyrivibrio* (HR=0.3537, 95% CI 0.1397-0.8957), or *Deinococcus* (HR=0.4763, 95% CI 0.2291-0.9901). Conversely, the risk was significantly higher for patients with higher abundance of *Microbacterium* (HR=2.632, 95% CI 1.113-6.224) (Fig. 5a-d).

Tumor microbiome function was significantly different between NRM and R/M patients

To determine whether the compositional differences between the two tumor microbiomes corresponded to functional differences, PICRUSt was used to predict the potential function of tumor microbiomes using 16S rRNA gene data. The top 20 most abundant level 2 and 3 KEGG pathways in the two different groups are shown in Fig. 6a,b. The comparison of enriched level 3 KEGG pathways between the two groups, based on the Dunn test, is shown in the Additional file 1: Table S5. In general, there were two level 3 KEGG pathways enriched in the NRM group and 69 in the R/M group. Genes associated with isoflavonoid biosynthesis and glycosylphosphatidylinositol-anchor biosynthesis were more abundant in NRM patients. However, genes associated with bacterial invasion of epithelial cells, cell division, steroid hormone biosynthesis, aminoacyl-tRNA biosynthesis, ECM-receptor interaction, and DNA replication were more abundant in R/M patients (adjusted $P < 0.05$, Dunn test; Additional file 1: Table S5).

Tumor DEGs between NRM and R/M patients

To investigate the differences in tumor gene expression at the transcriptional level, we performed transcriptome sequencing on total RNA samples from 26 NRM patients and 31 R/M patients, whose tumor microbiome DNA samples were used for 16S rRNA gene analyses. Overall, NRM and R/M groups had 22,221,601 and 21,832,153 reads on average, respectively (Additional file 1: Table S6). Using DESeq2, we identified 16 DEGs (adjusted $P < 0.05$, Benjamini-Hochberg correction; Fig. 7a,b; Additional file 1: Table S7). Of the 16 DEGs, 11 were upregulated in the R/M group (e.g. AKR1C3, CD36, AKR1C1, MEST, and NR1H3), and five were downregulated (EIF5B, ANKHD1-EIF4EBP3, PABPN1, RBM47 and KCNK6).

Using clusterProfiler, we carried out GO enrichment analysis on the DEGs. Using clusterProfiler and gage R packages, we conduct KEGG enrichment analysis on the DEGs. We were unable to obtain information about GO and KEGG enrichment because of the small number of DEGs.

Associations between tumor microbiome differences and DEGs

In order to elucidate how microbial abundance in breast tumors may influence prognosis, we considered correlations between nine microbial taxa and 16 DEGs (Fig. 8; Additional file 1: Table S9). The relative abundance of *Ruminococcus* (Spearman rho=0.337, *P*=0.01) positively correlated with the expression of RBM47. The relative abundance of *Anaerostipes* positively correlated with the expression of EIF5B (Spearman rho=0.364, *P* = 0.005), RBM47 (Spearman rho=0.387, *P*=0.003), and ANKHD1-EIF4EBP3 (Spearman rho=0.346, *P*=0.008). The relative abundance of *Weissella* positively correlated with the expression of PABPN1 (Spearman rho=0.268, *P*=0.044), EIF5B (Spearman rho=0.263, P=0.048), RBM47 (Spearman rho=0.294, *P*=0.026), and ANKHD1-EIF4EBP3 (Spearman rho=0.319, *P*=0.016). The relative abundance of *Butyrivibrio* positively correlated with the expression of RBM47 (Spearman rho=0.354, *P*=0.007) and ANKHD1-EIF4EBP3 (Spearman rho=0.339, *P*=0.01). The relative abundance of *Dechloromonas* positively correlated with the expression of ANKHD1-EIF4EBP3 (Spearman rho=0.294, *P*=0.026). The relative abundance of *Anaerococcus* positively correlated with the expression of PABPN1 (Spearman rho=0.354, *P*=0.007), EIF5B (Spearman rho=0.308, *P*=0.02), and RBM47 (Spearman rho=0.305, *P*=0.021), and negatively correlated with the expression of PLIN2 (Spearman rho=-0.29, *P*=0.028), VAMP5 (Spearman rho=-0.285, *P*=0.032), FOS (Spearman rho=-0.291, *P*=0.028), and TXNIP (Spearman rho=-0.393, *P*=0.003).

The relative abundance of *Thiothrix* negatively correlated with the expression of EIF5B (Spearman rho=-0.292, *P*=0.028) and RBM47 (Spearman rho=-0.276, *P*=0.038). The relative abundance of *Deinococcus* negatively correlated with the expression of CD36 (Spearman rho=-0.283, *P*=0.033), and positively correlated with the expression of EIF5B (Spearman rho=0.383, *P*=0.003), RBM47 (Spearman rho=0.310, *P*=0.019), and ANKHD1-EIF4EBP3 (Spearman rho=0.301, *P*=0.023).

Influence of tumor microbiome on the TIME in breast cancer

Next, we aimed to explore the role of the tumor microbiota on the local immune microenvironment and the natural history of the cancer. We used the CIBERSORT tool to examine the relative fractions of 22 TIIC types based on the gene expression profiling of tumor tissues, and we explored associations between relative microbial abundance and TIICs. Fig. 9 exhibits the relative proportions of the 22 TIIC subpopulation in tumor samples. The fractions of plasma cells, $CD8^+$ T cells, follicular helper T cells, gamma delta T cells, activated NK cells, M0 macrophages, M1 macrophages, activated mast cells, and eosinophils were higher in tumor tissue from NRM patients than in tumors from R/M patients (Fig. 10). Conversely, the fractions of memory B cells, naive $CD4^+$ T cells, resting memory $CD4^+$ T cells, resting NK cells, monocytes, M2 macrophages, resting dendritic cells, activated dendritic cells, resting mast cells, and neutrophils were lower in tumor tissues from NRM patients (Fig. 10).

Next, associations between the tumor microbiome and the 22 TIIC types were analyzed to confirm the two-way relationship (Fig. 11; Additional file 1: Table S10). The relative abundance of *Dechloromonas* positively correlated with the fraction of activated mast cells (Spearman rho=0.268, *P*=0.044), while it negatively correlated with the fraction of resting mast cells (Spearman rho=-0.33, *P*=0.012). The relative abundances of *Weissella* (Spearman rho =-0.279, *P*=0.036) and *Anaerostipes* (Spearman rho =-0.279, *P*=0.036) negatively correlated with the fraction of gamma delta T cells. A trend towards a positive correlation was observed between the relative abundance of *Butyrivibrio* and the fraction of activated NK cells (Spearman rho=0.258, *P*=0.052).

Discussion

In our study, we explored the influence of the tumor microbiome on the prognosis of breast cancer. We performed a comprehensive comparison of the tumor microbiome between R/M and NRM breast cancer patients. We analyzed tumor microbiomes in terms of taxonomic profile and function, and established associations with tumor DEGs and TIICs. Overall, we detected a substantial microbiome in breast tumors, as previously reported [23, 46]. We found that tumor bacterial diversity was higher in the NRM group than in the R/M group. Furthermore, the NRM and R/M groups had different tumor microbiome signatures, with certain bacterial genera that were predictive of DFS. We also observed that differences in the tumor microbiome were associated with differences in TIIC subpopulations. We therefore hypothesize that tumor microbiota may play an important role in the natural history of breast cancer by influencing the local immune microenvironment.

Several bacterial genera were found to be less abundant in R/M relative to NRM patients: *Ruminococcus, Anaerostipes*, *Weissella, Butyrivibrio*, and *Deinococcus. Ruminococcus* [47, 48] and *Butyrivibrio* [49] have been reported to produce butyrate. Butyrate acts as an antitumorigenic and antiproliferative agent, due to its regulation of genes that decrease cell proliferation and its ability to induce apoptosis by inhibiting histone deacetylases [50]. Moreover, studies suggest that microbially produced butyrate regulates the differentiation of T cells [51]. Immune cell function has also been extensively linked to progression of breast cancer [25–27]. The reduction of butyrate may influence the differentiation of T cells and increase the possibility of breast cancer progression. This is supported by our observation that the proportions of $CD8^+$ and follicular helper T cells were lower in tumor tissues of R/M patients than in tumors of NRM patients. This may be because R/M patients had lower abundance of butyrate-producing bacteria, which correlated with significantly worse prognosis.

The R/M group presented higher relative abundances of *Dechloromonas, Anaerococcus, Thiothrix*, and *Microbacterium* than the NRM group. *Anaerococcus* is a member of the Gram-positive anaerobic cocci able to induce inflammation, remodeling of the extracellular matrix (ECM) and re-epithelialization [52]. The promotion of inflammation and remodeling of the ECM results in mutagenesis that may promote the onset and progression of cancer [53]. Studies have shown that *Anaerococcus* is involved in progression of cervical intraepithelial neoplasia [54, 55] and bladder cancer [56]. Therefore, the increase of *Anaerococcus* may be related to progression of breast cancer.

Differences in tumor microbial composition likely translate into differences in tumor microbial function. Genes involved in steroid hormone biosynthesis and ECM-receptor interaction were more abundant in R/M patients. Breast cancer is hormone-dependent: steroid hormones play a key role in breast cancer onset and progression [57], and these hormones exert their mitogenic effects by binding to estrogen, progesterone, and androgen receptors [58]. Several studies have shown that the ECM-receptor signaling pathway plays a crucial role in modulating breast cancer metastasis [59–62]. Therefore, enrichment of steroid hormone biosynthesis and ECM-receptor interaction in R/M patients may promote breast cancer progression.

In order to begin explaining how differences in tumor microbiome composition may influence prognosis, we correlated differences in microbial abundance to DEGs between R/M and NRM patients. We observed a negative correlation between the relative abundance of *Deinococcus*, a predictor for better prognosis in breast cancer patients in our study, and expression of CD36, which plays a critical role in proliferation and migration of breast cancer cells [63]. These findings indicate that the interactions between host gene expression and microbiome may be involved in the progression of breast cancer.

We analyzed the composition of TIICs between the two patient groups in order to explore the influence of the tumor microbiota on the local immune microenvironment and the natural history of the cancer. We observed the differences of composition of TIICs between the two patient groups. And we discovered that the relative abundances of *Anaerostipes* and *Weissella* were negatively correlated with the fractions of gamma delta T cells, which has been associated with longer DFS in breast cancer [64, 65]. Furthermore, the relative abundance of *Dechloromonas* was positively correlated with the fraction of activated mast cells, previously associated with good prognosis in breast cancer [66–69]. In addition, we observed a trend for a positive correlation between *Butyrivibrio* and activated NK cells, which are involved in inhibiting the growth and metastasis of tumors [70–72]. These results are consistent with reports showing that the numbers of natural killer cells markedly increase in response to *Butyrivibrio fibrisolvens* (the main member of *Butyrivibrio*) [73], and that increased numbers of natural killer cells may contribute to the alleviation of carcinogenesis by *B. fibrisolvens* [74]. This is supported by our observations, since breast cancer patients with more abundant *Butyrivibrio* showed better prognosis.

Conclusion

In summary, we provide evidence that the tumor microbiome is associated with prognosis of breast cancer patients. The tumor microbiome may influence the TIME and thereby influence risk of recurrence or metastasis. Thus, the tumor microbiome may be a useful prognostic indicator in breast cancer.

Abbreviations

NRM: Without recurrence or metastasis; R/M:Relapse or metastasis; DEGs:Differentially expressed genes; TIICs:Tumor-infiltrating immune cells; ASVs:Amplicon sequence variants; PERMANOVA:Permutational multivariate analysis of variance; PCoA:Principal coordinate analyses; PLS-DA:Partial least squares

discriminant analysis; ROC:Receiver operating characteristic; PICRUSt:Phylogenetic investigation of communities by reconstruction of unobserved states; GO:Gene ontology; KEGG:Kyoto encyclopedia of genes and genomes; $\bar{x}$:mean; sd:Standard deviation; BMI:Body mass index; DFS:Disease-free survival; HER2:Human epidermal growth factor receptor 2.

Declarations

Ethical approval and consent to participate

The study was approved by the Ethics Committee of the First Affiliated Hospital of Nanchang University, Nanchang, Jiangxi, China and informed consent was obtained from all subjects.

Consent for publication

Not applicable.

Availability of data and materials

The raw data has been uploaded on NCBI portal at Sequence Read Archive (SRA) BioProject ID: PRJNA667135 and PRJNA667027. 16S rRNA microbiome data-Submission ID: SUB8231639 and RNA-Seq data-Submission ID: SUB8241353. The raw data hasn't been released.

Competing interests

The authors declare that they have no competing interests.

Funding

This study was supported by the Youth Science Fund Project of Jiangxi Provincial Department of Science and Technology (20192BAB215037), the Science and Technology Project of Education Department of Jiangxi Province (GJJ180057) and the Science and Technology Project of Education Department of Jiangxi Province (GJJ180056).

Authors’ contributions

BW, JZ, and XGT designed the study. JZ performed the data analysis and wrote the manuscript. JW, CGM and SYL performed the data analysis. TL, TTQ, XTY, and RBQ performed telephone interviews and collected clinical data. All authors read and approved the final manuscript.

Acknowledgements

We thank Yanyang Liu, Shuyao Jiang and Chunxia fan for technical assistance. We thank Microeco Tech Co., Ltd. Shenzhen China for sequencing service and assistance.

References

1. Cho I, Blaser MJ. The human microbiome: at the interface of health and disease. Nat Rev Genet. 2012;13:260–70.
2. Sawyers CL, Abate-Shen C, Anderson KC, Barker A, Baselga J, Berger NA, et al. AACR Cancer Progress Report 2013. Clin Cancer Res. 2013; 19:S4–98.
3. Martel CD, Ferlay J, Franceschi S, Vignat J, Bray F, Forman D, et al. Global burden of cancers attributable to infections in 2008: a review and synthetic analysis. Lancet Oncol. 2012; 13:607–15.
4. Bhatt AP , Redinbo MR , Bultman SJ . The role of the microbiome in cancer development and therapy. CA Cancer J Clin. 2017;67:326–44.
5. Kuper H, Adami HO, Trichopoulos D. Infections as a major preventable cause of human cancer. J Intern Med. 2000;248:171–83.
6. Kundu JK , Surh YJ. Inflammation: gearing the journey to cancer. Mutat Res. 2008;659:15-30.
7. Kostic AD , Gevers D, Pedamallu CS, Michaud M, Duke F, Earl AM, et al. Genomic analysis identifies association of Fusobacterium with colorectal carcinoma. Genome Res. 2012;22:292-98.
8. Wotherspoon AC, Doglioni C, Diss TC, Pan L, Moschini A, de Boni M, et al. Regression of primary low-grade B-cell gastric lymphoma of mucosa-associated lymphoid tissue type after eradication of Helicobacter pylori. Lancet. 1993;342:575-7.
9. Forman D, Newell DG, Fullerton F, Yarnell J W, Stacey A R, Wald N, et al. Association between infection with Helicobacter pylori and risk of gastric cancer: evidence from a prospective investigation. BMJ. 1991;302:1302-5.
10. Uemura N, Okamoto S, Yamamoto S, Matsumura N, Yamaguchi S, Yamakido M, et al. Helicobacter pylori infection and the development of gastric cancer. N Engl J Med. 2001;345:784-9.
11. Ahn J, Sinha R, Pei Z, Dominianni C, Wu J, Shi J, et al. Human gut microbiome and risk for colorectal cancer. J Natl Cancer Inst. 2013;105:1907-11.
12. Schwabe RF , Jobin C. The microbiome and cancer. Nat Rev Cancer. 2013; 13:800-12.
13. Crusz SM, Balkwill FR. Inflammation and cancer: advances and new agents. Nat Rev Clin Oncol. 2015;12:584-96.
14. Hunt KM , Foster JA, Forney LJ, Schütte UME, Beck DL, Abdo Z, et al. Characterization of the diversity and temporal stability of bacterial communities in human milk. PLoS One. 2011;6: e21313.
15. Cabrera-Rubio R , Collado MC, Laitinen K, Salminen S, Isolauri E, Mira A. The human milk microbiome changes over lactation and is shaped by maternal weight and mode of delivery. Am J Clin Nutr. 2012;96:544-51.
16. Going JJ , Moffat DF. Escaping from Flatland: clinical and biological aspects of human mammary duct anatomy in three dimensions. J Pathol. 2004;203:538-44.
17. Maqsood R, Rodgers R, Rodriguez C, Handley SA, Ndao IM, Tarr PI, et al. Discordant transmission of bacteria and viruses from mothers to babies at birth. Microbiome. 2019;7:156.

18. Stinson LF, Sindi ASM, Cheema AS, Lai CT, Mühlhäusler BS, Wlodek ME, et al. The human milk microbiome: who, what, when, where, why, and how? Nutr Rev 2020:1–18
19. Asnicar F, Manara S, Zolfo M, Truong DT, Scholz M, Armanini F, et al. Studying Vertical Microbiome Transmission from Mothers to Infants by Strain-Level Metagenomic Profiling. mSystems. 2017;2:e00164-16
20. Jost T, Lacroix C, Braegger CP, Rochat F, Chassard C. Vertical mother–neonate transfer of maternal gut bacteria via breastfeeding. Environ Microbiol. 2014; 16:2891–904
21. Hieken TJ, Chen J, Hoskin TL, Walther-Antonio M, Johnson S, Ramaker S, et al. The Microbiome of Aseptically Collected Human Breast Tissue in Benign and Malignant Disease. Sci Rep. 2016;6:30751.
22. Urbaniak C, Cummins J, Brackstone M, Macklaim JM, Gloor GB, Baban CK, et al. Microbiota of human breast tissue. Appl Environ Microbiol. 2014;80:3007-14.
23. Urbaniak C, Gloor GB, Brackstone M, Scott L, Tangney M, Reid G,et al. The microbiota of breast tissue and its association with breast cancer. Appl Environ Microbiol. 2016;82:5039-48.
24. Degnim AC, Brahmbhatt RD, Radisky DC, Hoskin TL, Stallings-Mann M, Mark Laudenschlager, et al. Immune cell quantitation in normal breast tissue lobules with and without lobulitis. Breast Cancer Res Treat. 2014;144:539-49.
25. DeNardo DG, Barreto JB, Andreu P, Vasquez L, Tawfik D, Kolhatkar N, et al. CD4(+) T cells regulate pulmonary metastasis of mammary carcinomas by enhancing protumor properties of macrophages. Cancer Cell. 2009;16:91–102.
26. Bingle L, Lewis CE, Corke KP, Reed MW, Brown NJ. Macrophages promote angiogenesis in human breast tumour spheroids in vivo. Br J Cancer. 2006; 94:101–7.
27. DeNardo DG, Brennan DJ, Rexhepaj E, Ruffell B, Shiao SL, Madden SF, et al. Leukocyte complexity predicts breast cancer survival and functionally regulates response to chemotherapy. Cancer Discov. 2011;1:54–67.
28. Callahan BJ, McMurdie PJ, Rosen MJ, Han AW, Johnson AJ, Holmes SP. DADA2:high-resolution sample inference from Illumina amplicon data. Nat Methods. 2016;13:581–3.
29. Bokulich NA, Kaehler BD, Rideout JR, Dillon M, Bolyen E, Knight R, et al. Optimizing taxonomic classification of marker-gene amplicon sequences with QIIME 2 ' s q2-feature-classifier plugin. Microbiome. 2018;6:90.
30. Segata N, Izard J, Waldron L, Gevers D, Miropolsky L, Garrett WS, et al. Metagenomic Biomarker Discovery and Explanation." Genome biology. 2011; 12: R60.
31. Vázquez-Baeza Y, Pirrung M, Gonzalez A, Knight R. Emperor: a tool for visualizing high-throughput microbial community data. Gigascience. 2013;2:16.
32. Rohart F, Gautier B, Singh, A, Cao KL. mixOmics: An R package for 'omics feature selection and multiple data integration. PLoS Comput Biol. 2017;13:e1005752.
33. Langille MG, Zaneveld J, Caporaso JG, McDonald D, Knights D, Reyes JA, et al. Predictive functional profiling of microbial communities using 16s rrna marker gene sequences. Nat Biotechnol.

2013;31:814-21.
34. Dunn OJ. Multiple comparisons among means. J Am Stat Assoc. 1961;56:52–64.
35. Mortazavi A, Williams BA, McCue K, Schaeffer L, Wold B. Mapping and quantifying mammalian transcriptomes by RNA-Seq. Nat Methods. 2008;5:621-28.
36. Pertea M, Pertea GM, Antonescu CM, Chang TC, Mendell JT, Salzberg SL. StringTie enables improved reconstruction of a transcriptome from RNA-seq reads, Nat Biotechnol 2015; 33:290-5.
37. Bray NL, Pimentel H, Melsted P, Pachter L. Near-optimal probabilistic RNA-seq quantification. Nat Biotechnol. 2016;34:525-7.
38. Anders S, Huber W. Differential expression analysis for sequence count data. Genome Biol. 2010; 11:R106.
39. Love MI, Huber W, Anders S. Moderated estimation of fold change and dispersion for RNA-seq data with DESeq2. Genome Biol. 2014;15:550.
40. Young MD, Wakefield MJ, Smyth GK, Oshlack A. Gene ontology analysis for RNA-seq:accounting for selection bias. Genome Biol. 2010;11: R14.
41. Luo W, Friedman MS, Shedden K, Hankenson KD, Woolf PJ. GAGE: generally applicable gene set enrichment for pathway analysis. BMC Bioinformatics. 2009;10: 161.
42. Chen B, Khodadoust MS, Liu CL, Newman AM, Alizadeh AA. Profiling Tumor Infiltrating Immune Cells with CIBERSORT. Methods Mol Biol. 2018;1711:243–59.
43. Zhang E, Dai F, Mao Y, He W, Liu F, Ma W, et al. Differences of the immune cell landscape between normal and tumor tissue in human prostate. Clin Transl Oncol. 2020; 22:344–50.
44. Ali HR, Chlon L, Pharoah PDP, Markowetz F, Caldas C. Patterns of immune infiltration in breast cancer and their clinical implications: a gene-expression-based retrospective study. PLoS Med. 2016;13:e1002194
45. Liu X, Wu S, Yang Y, Zhao M, Zhu G, Hou Z. The prognostic landscape of tumor-infiltrating immune cell and immunomodulators in lung cancer. Biomed Pharmacother. 2017;95:55–61.
46. Xuan C, Shamonki JM, Chung A, Dinome ML, Chung M, Sieling PA, et al. Microbial Dysbiosis Is Associated with Human Breast Cancer. PLoS One. 2014;9:e83744.
47. Takahashi K, Nishida A, Fujimoto T, Fujii M, Shioya M, Imaeda H, et al. Reduced Abundance of Butyrate-Producing Bacteria Species in the Fecal Microbial Community in Crohn's Disease. Digestion. 2016;93:59-65.
48. Liu F, Li P, Chen M, Luo YM, Prabhakar M, Zheng HM, et al. Fructooligosaccharide (FOS) and Galactooligosaccharide (GOS) Increase Bifidobacterium but Reduce Butyrate Producing Bacteria with Adverse Glycemic Metabolism in healthy young population. Sci Rep. 2017;7:11789.
49. Anand S, Kaur H, Mande SS. Comparative In silico Analysis of Butyrate Production Pathways in Gut Commensals and Pathogens. Front Microbiol. 2016;7:1945.
50. Chang PV, Hao L, Offermanns S, Medzhitov R. The microbial metabolite butyrate regulates intestinal macrophage function via histone deacetylase inhibition. Proc Natl Acad Sci USA. 2014; 111:2247-52.

51. Furusawa Y, Obata Y, Fukuda S, Endo TA, Nakato G, Takahashi D, et al. Commensal microbe-derived butyrate induces the differentiation of colonic regulatory T cells. Nature. 2013;504:446-50.
52. Murphy E C, Frick IM. Gram-positive anaerobic cocci–commensals and opportunistic pathogens. FEMS Microbiol Rev. 2013;37:520–53.
53. Alfano M, Canducci F, Nebuloni M, Clementi M, Montorsi F, Salonia A. The interplay of extracellular matrix and microbiome in urothelial bladder cancer. Nat Rev Urol. 2016;13:77-90.
54. Chen YL, Qiu XD, Wang WJ, Li D, Wu AY, Hong ZB, et al. Human papillomavirus infection and cervical intraepithelial neoplasia progression are associated with increased vaginal microbiome diversity in a Chinese cohort. BMC Infect Dis. 2020;20:629.
55. Mitra A, MacIntyre DA, Lee YS, Smith A, Marchesi JR, Lehne B, et al. Cervical intraepithelial neoplasia disease progression is associated with increased vaginal microbiome diversity. Sci Rep. 2015;5:16865.
56. Wu P, Zhang G, Zhao J, Chen J, Chen Y, Huang W, et al. Profiling the Urinary Microbiota in Male Patients With Bladder Cancer in China. Front Cell Infect Microbiol. 2018;8:167.
57. Cheng M, Michalski S, Kommagani R. Role for Growth Regulation by Estrogen in Breast Cancer 1 (GREB1) in Hormone-Dependent Cancers. Int J Mol Sci. 2018;19:2543.
58. Africander D, Storbeck KH. Steroid metabolism in breast cancer: Where are we and what are we missing? Mol Cell Endocrinol. 2018;466:86-97.
59. Huan JL, Gao X, Xing L, Qin XJ, Qian HX, Zhou Q, et al. Screening for key genes associated with invasive ductal carcinoma of the breast via microarray data analysis. Genet Mol Res. 2014;13:7919-25.
60. Schwertfeger KL, Cowman MK, Telmer PG, Turley EA, McCarthy JB. Hyaluronan, Inflammation, and Breast Cancer Progression. Front Immunol. 2015;6:236.
61. Tolg C, McCarthy JB, Yazdani A, Turley EA. Hyaluronan and RHAMM in wound repair and the "cancerization" of stromal tissues. Biomed Res Int. 2014; 2014:103923.
62. Yeh MH, Tzeng YJ, Fu TY, You JJ, Chang HT, Ger LP, et al. Extracellular Matrix–receptor Interaction Signaling Genes Associated with Inferior Breast Cancer Survival. Anticancer Res. 2018;38:4593-605.
63. Liang Y, Han H, Liu LP, Duan YJ, Yang XX, Ma CR, et al. CD36 plays a critical role in proliferation, migration and tamoxifen-inhibited growth of ER-positive breast cancer cells. Oncogenesis. 2018;7:98.
64. Gentles AJ, Newman AM, Liu CL, Bratman SV, Feng WG, Kim DK, et al. The prognostic landscape of genes and infiltrating immune cells across human cancers. Nat Med. 2015;21:938-45..
65. Bense RD, Sotiriou C, Piccart-Gebhart MJ, Haanen JBAG, van Vugt MATM, de Vries EGE, et al. Relevance of Tumor-Infiltrating Immune Cell Composition and Functionality for Disease Outcome in Breast Cancer. J Natl Cancer Inst. 2016;109:djw192.
66. Aaltomaa S, Lipponen P, Palpinaho S, Kosma VM. Mast cells in breast cancer. Anticancer Res. 1993;13:785–8.

67. Dabiri S, Huntsman D, Makretsov N, Cheang M, Gilks B, Bajdik C, et al. The presence of stromal mast cells identifies a subset of invasive breast cancers with a favorable prognosis. Mod Pathol. 2004;17:690–95.
68. Rajput A, Turbin D, Cheang MC, Voduc DK, Leung S, Gelmon KA, et al. Stromal mast cells in invasive breast cancer are a marker of favourable prognosis: A study of 4,444 cases. Breast Cancer Res Treat. 2008;107:249–57.
69. Rovere F Della, Granata A, Familiari D, D'Arrigo G, Mondello B, Basile G. Mast cells in invasive ductal breast cancer: Different behavior in high and mini-mum hormone-receptive cancers. Anticancer Res. 2007;27:2465–71.
70. Moretta L. NK cell-mediated immune response against cancer. Surg Oncol. 2007; 16:S3–5.
71. Ames IH, Garcia AM, John PA, Litty CA, Farrell MA, Tomar RH. Decreased natural cytotoxicity in mice with high incidence of mammary adenocarcinoma. Clin Immunol Immunopathol. 1986;38:265–73.
72. Cook JL, Lewis AM Jr. Immunological surveillance against DNA-virus-transformed cells: correlations between natural killer cell cytolytic competence and tumor susceptibility of athymic rodents. J Virol. 1987;61:2155–61.
73. Ohkawara S, Furuya H, Nagashima K, Asanuma N, Hino T. Oral administration of butyrivibrio fibrisolvens, a butyrate-producing bacterium, decreases the formation of aberrant crypt foci in the colon and rectum of mice. J Nutr. 2005;135:2878-83.
74. Ohkawara S, Furuya H, Nagashima K, Asanuma N, Hino T. Effect of oral administration of Butyrivibrio fibrisolvens MDT-1, a gastrointestinal bacterium, on 3-methylcholanthrene-induced tumor in mice. Nutr Cancer. 2007;59:92-8.

Tables

Table 1. Demographic and clinical characteristics of the study patients.

Characteristic	NRM (n=26)	R/M (n=31)	*P* value
Age ($\bar{x}$±sd)	51.31±11.99	50.94±9.24	0.895
BMI ($\bar{x}$± sd)	22.36±2.07	22.68±3.16	0.67
Ethnicity			
Han	26	30	1.000
Non- Han	0	1	
DFS (months) ($\bar{x}$±sd)	84.46±10.04	23.35±22.2	**<0.001**
Cancer stage			
IIA	4	5	0.275
IIB	8	4	
IIIA	6	5	
IIIB	1	5	
IIIC	7	12	
Neoadjuvant chemotherapy			
Yes	5	9	0.392
No	21	22	
Antibiotics (pre-surgery)			
Yes	4	2	0.274
No	22	29	
Molecular subtype			
Luminal A	5	4	0.59
Luminal B	11	11	
HER2- enriched	9	12	
Basal-like	1	4	

Abbreviations: NRM, without recurrence or metastasis : R/M, relapse or metastasis; $\bar{x}$, mean; sd, standard deviation; BMI, body mass index; DFS, disease-free survival; HER2, human epidermal growth factor receptor 2.

Figures

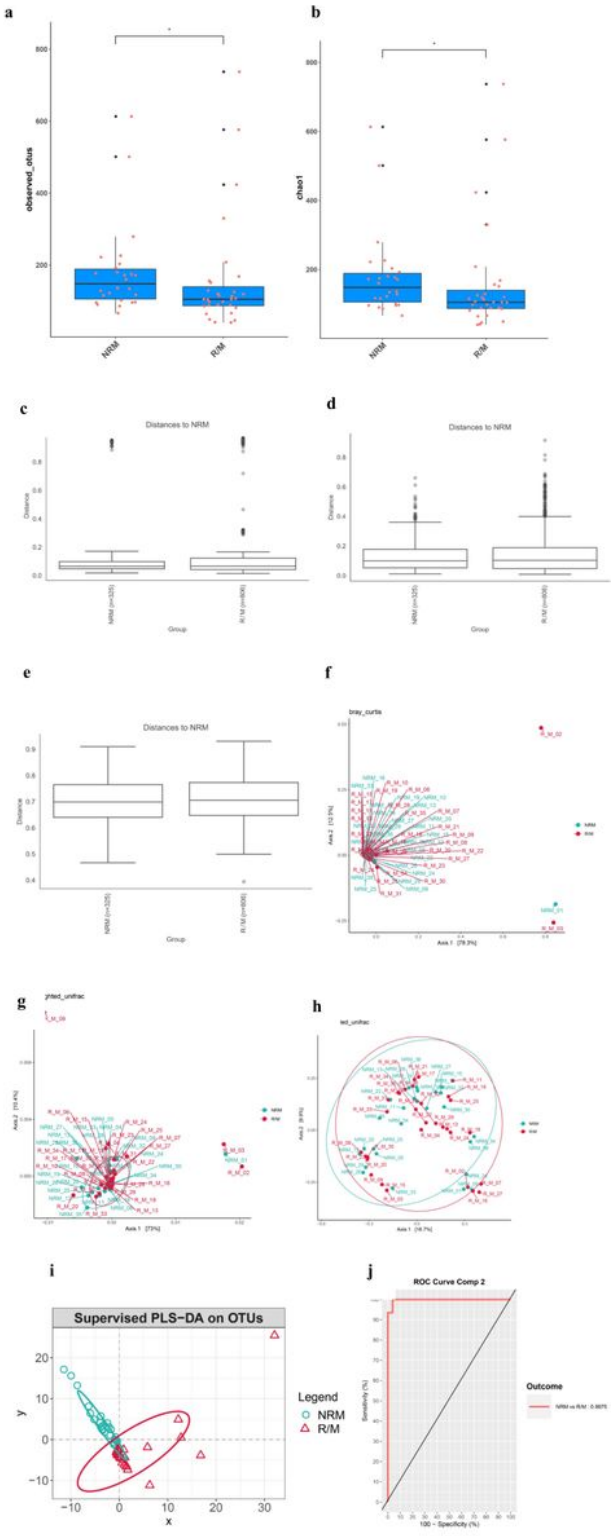

Figure 1

Comparison of microbiome alpha and beta diversity between patients experiencing no recurrence or metastasis (NRM) and patients experiencing recurrence or metastasis (R/M). a Observed OTUs index. b Chao1 index. c Bray-Curtis distance index. d Weighted UniFrac index. e Unweighted UniFrac distance index. f Principal coordinate analysis (PCoA) of Bray-Curtis metrics. g PCoA of weighted UniFrac matrix. h PCoA of unweighted UniFrac matrix. i Partial least squares discriminant analysis (PLS-DA) on OTUs

between the NRM and R/M groups. j Receiver operating characteristic (ROC) curve analysis for the predictive value of the model constructed based on the PLS-DA analysis. The area under the curve (AUC) of the NRM and R/M groups was 0.9975. *P<0.05

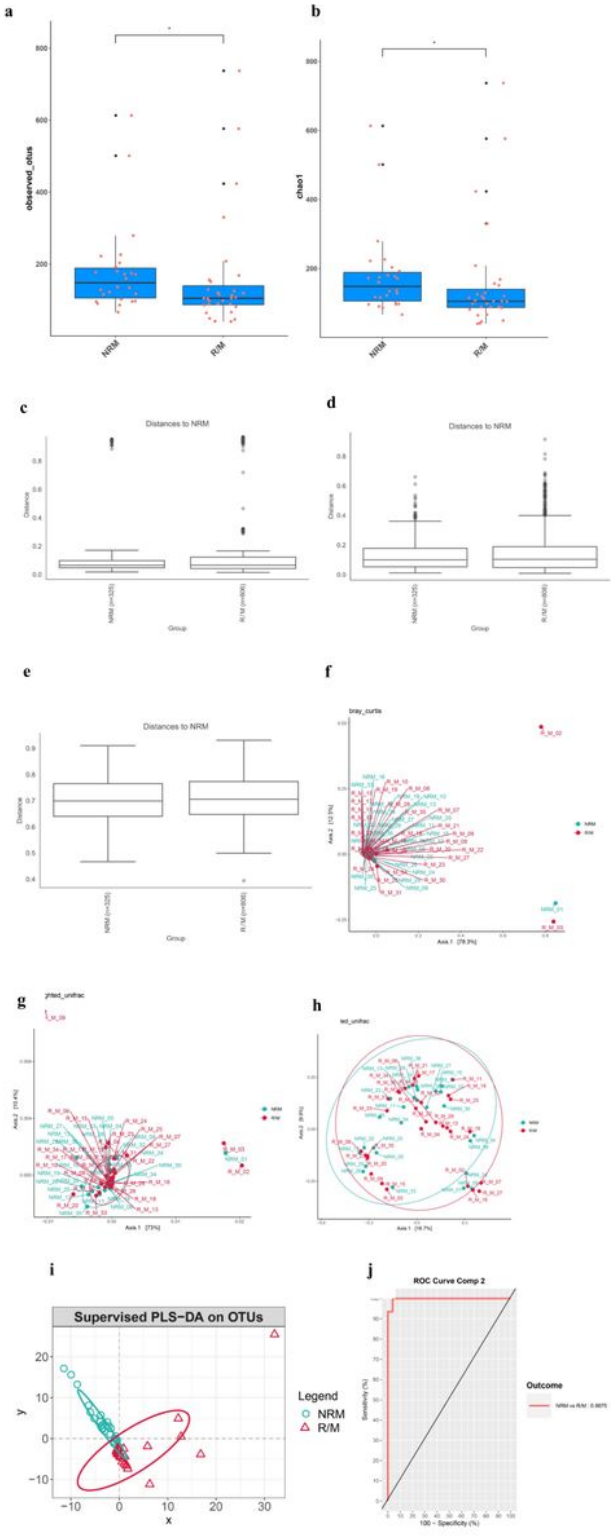

Figure 1

Comparison of microbiome alpha and beta diversity between patients experiencing no recurrence or metastasis (NRM) and patients experiencing recurrence or metastasis (R/M). a Observed OTUs index. b

Chao1 index. c Bray-Curtis distance index. d Weighted UniFrac index. e Unweighted UniFrac distance index. f Principal coordinate analysis (PCoA) of Bray-Curtis metrics. g PCoA of weighted UniFrac matrix. h PCoA of unweighted UniFrac matrix. i Partial least squares discriminant analysis (PLS-DA) on OTUs between the NRM and R/M groups. j Receiver operating characteristic (ROC) curve analysis for the predictive value of the model constructed based on the PLS-DA analysis. The area under the curve (AUC) of the NRM and R/M groups was 0.9975. *P<0.05

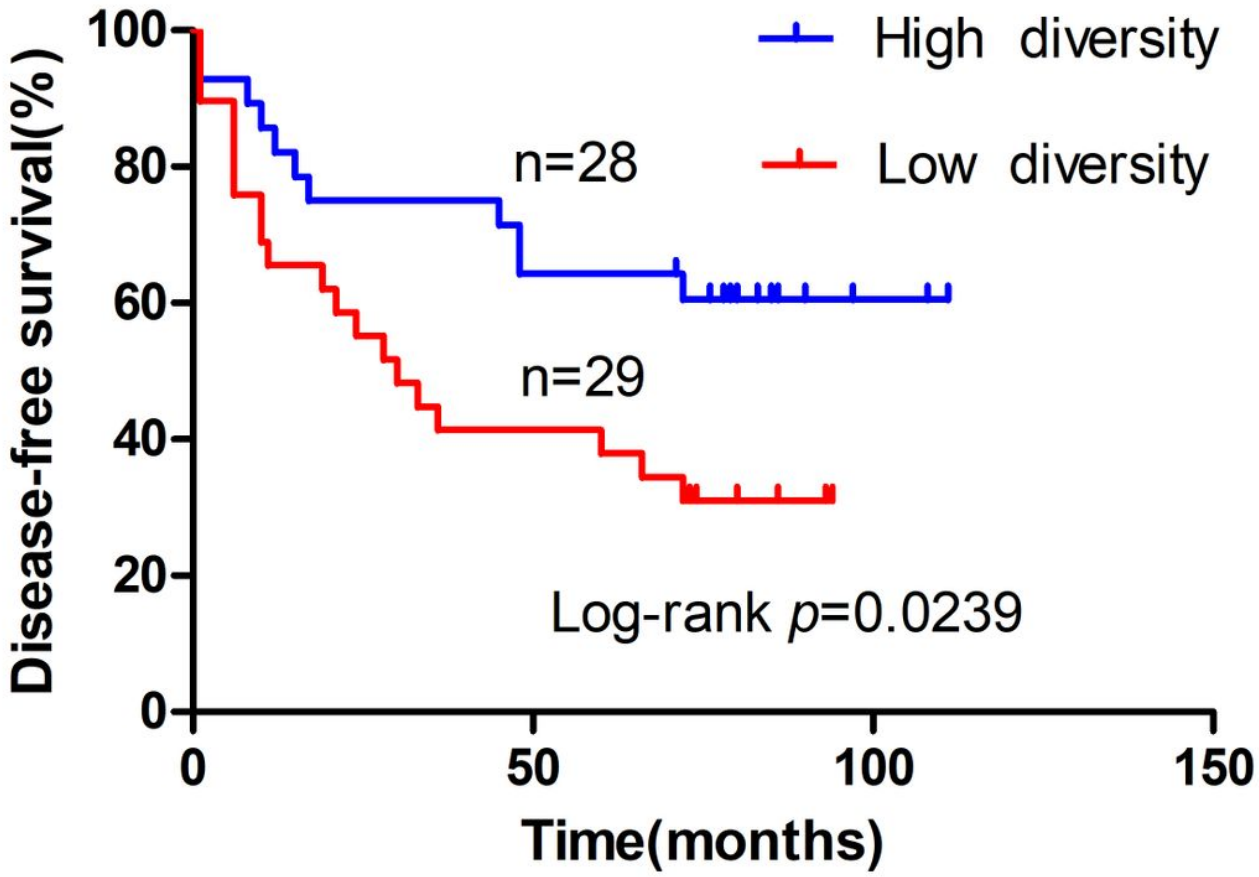

Figure 2

Kaplan-Meier estimates for disease-free survival (DFS) defined by alpha diversity in no recurrence or metastasis (NRM) and recurrence or metastasis (R/M) groups.

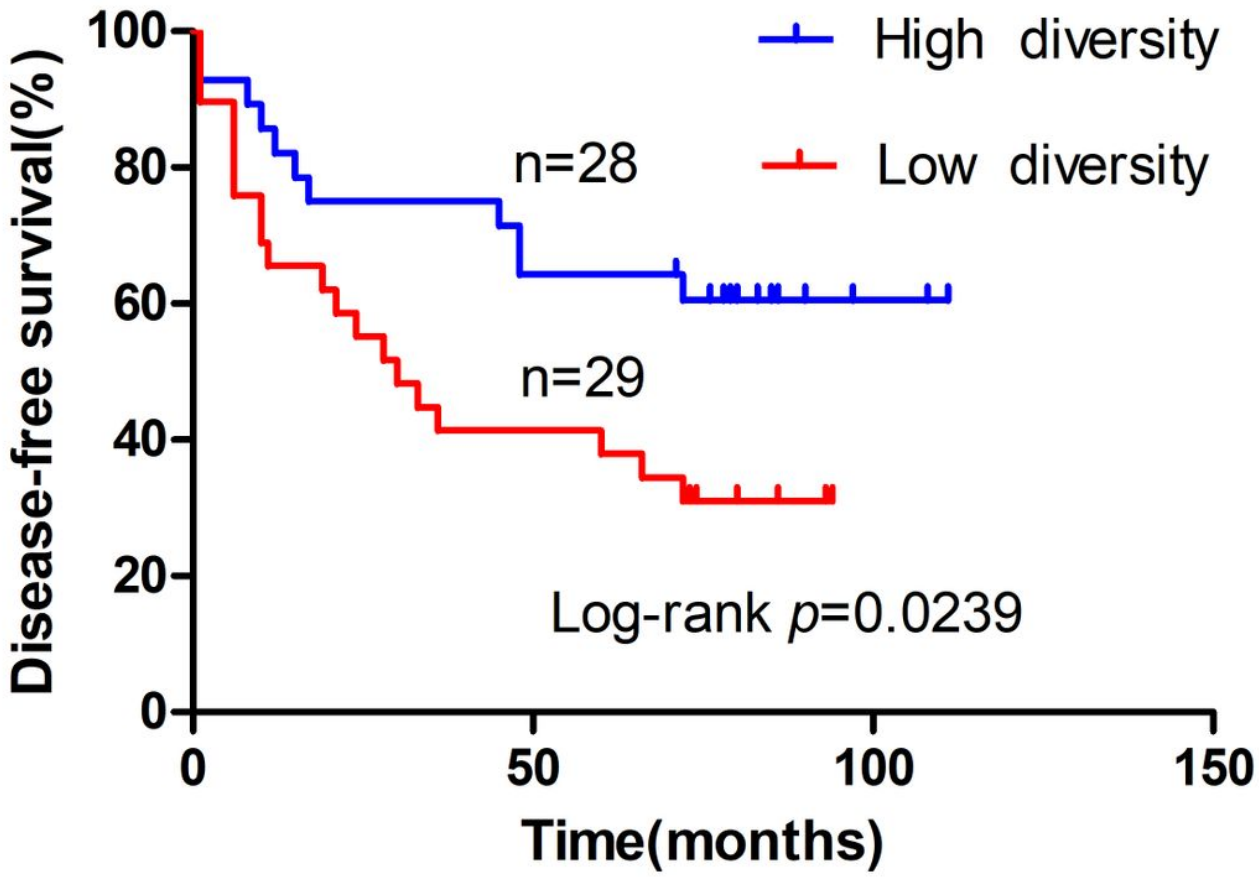

Figure 2

Kaplan-Meier estimates for disease-free survival (DFS) defined by alpha diversity in no recurrence or metastasis (NRM) and recurrence or metastasis (R/M) groups.

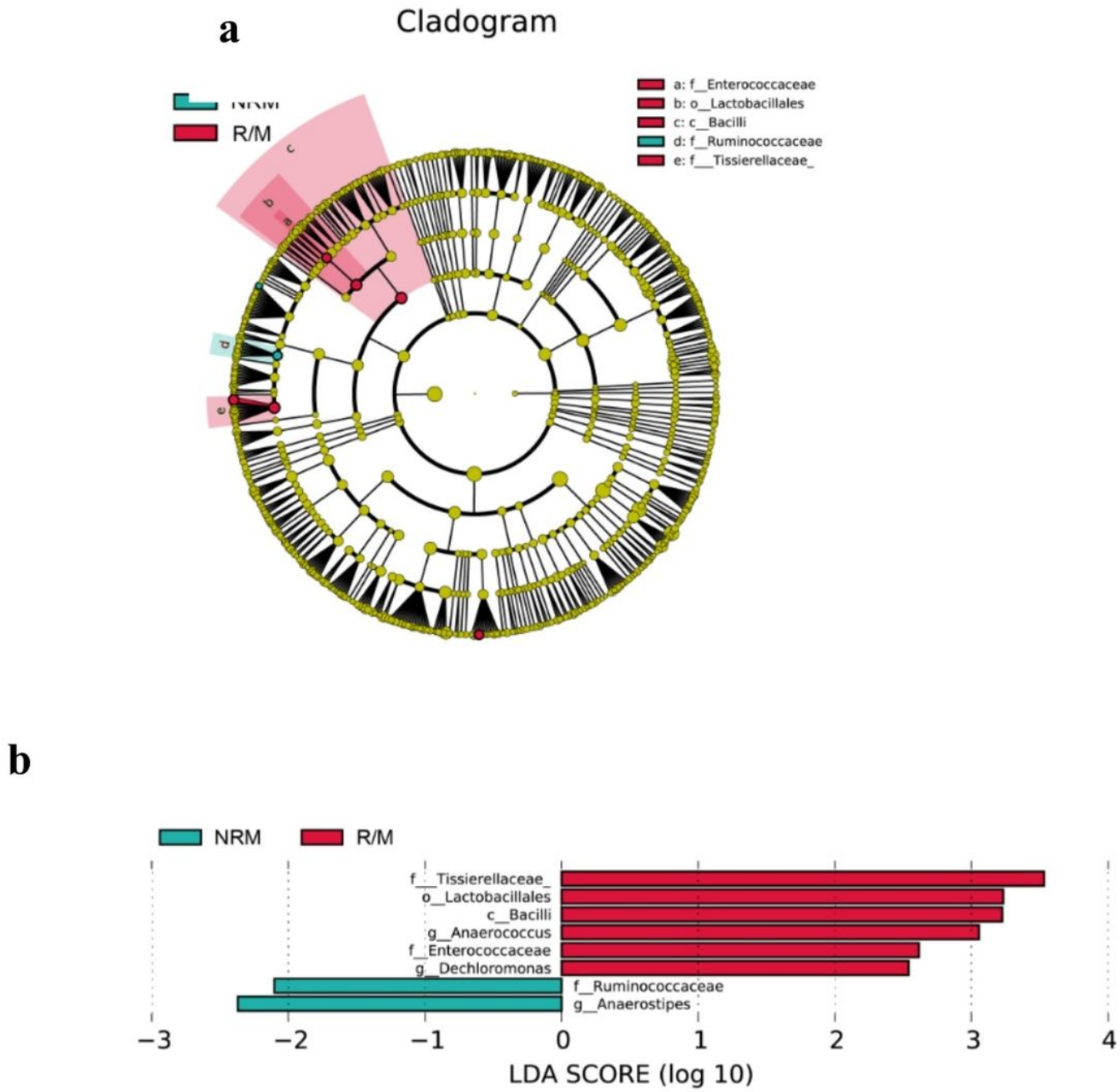

Figure 3

Linear discrimination analysis (LDA) effect size (LEfSe) analysis revealed differentially abundant taxa between patients with no recurrence or metastasis (NRM) and patients with recurrence or metastasis (R/M). a Cladogram showing the different taxonomic composition in the two groups. Differences are represented by the color of the most abundant class (red, R/M group; green, NRM group; yellow, insignificant). Each ring represents a specific taxonomic level. b LDA score computed from features differentially abundant between NRM and R/M patients (green, NRM group; red, R/M group). The criteria for feature selection was LDA > 2.

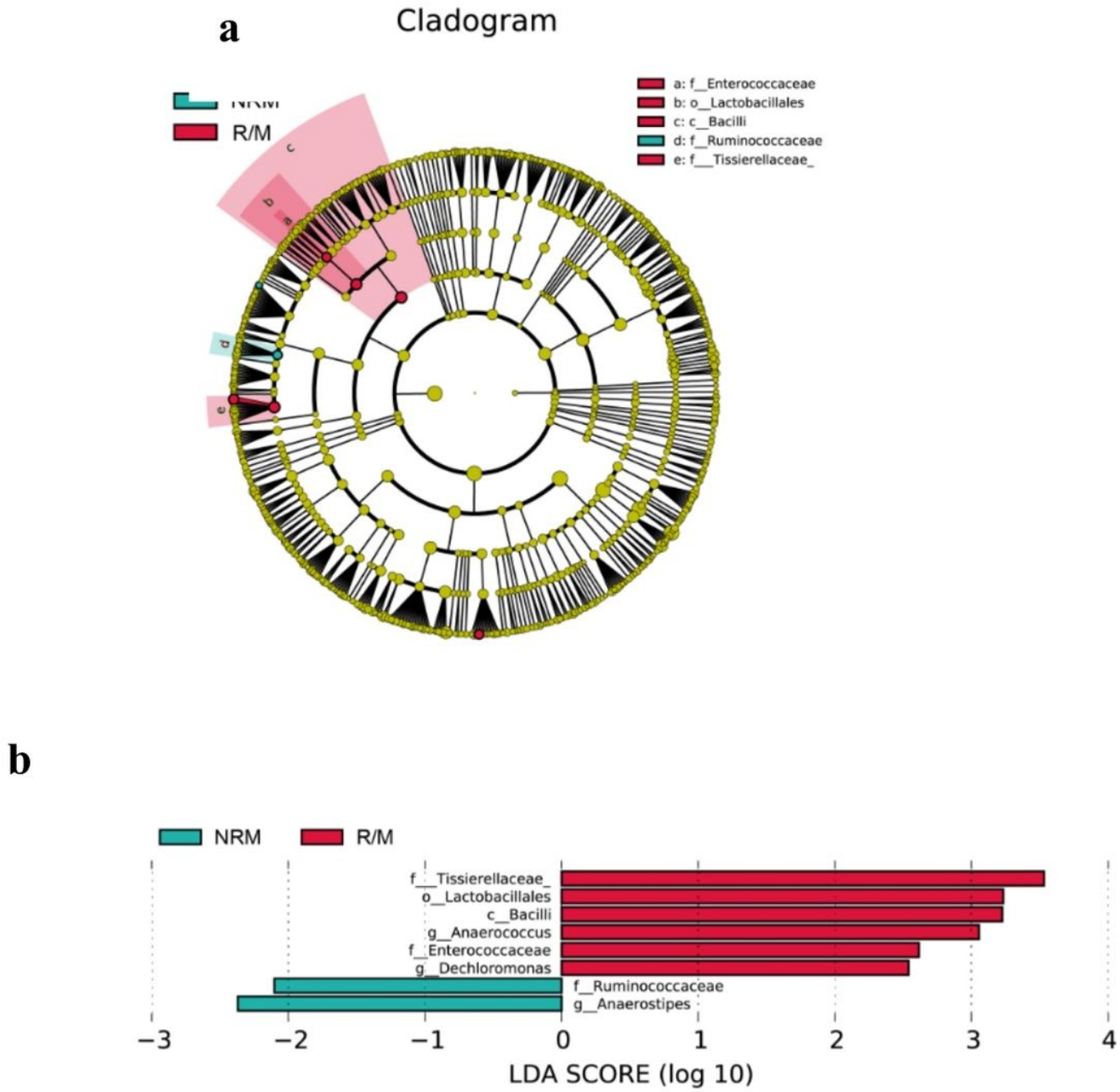

Figure 3

Linear discrimination analysis (LDA) effect size (LEfSe) analysis revealed differentially abundant taxa between patients with no recurrence or metastasis (NRM) and patients with recurrence or metastasis (R/M). a Cladogram showing the different taxonomic composition in the two groups. Differences are represented by the color of the most abundant class (red, R/M group; green, NRM group; yellow, insignificant). Each ring represents a specific taxonomic level. b LDA score computed from features differentially abundant between NRM and R/M patients (green, NRM group; red, R/M group). The criteria for feature selection was LDA > 2.

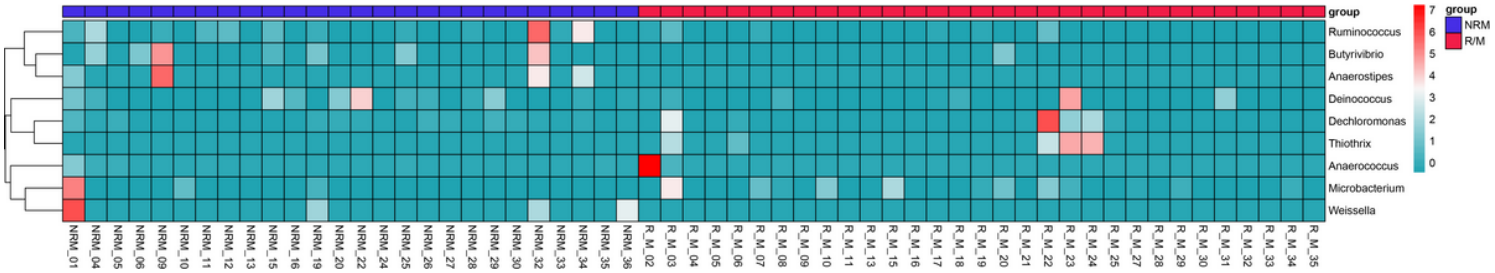

Figure 4

Heatmap of tumor microbiome differences at genus level between patients experiencing no recurrence or metastasis (NRM) and patients experiencing recurrence or metastasis (R/M).

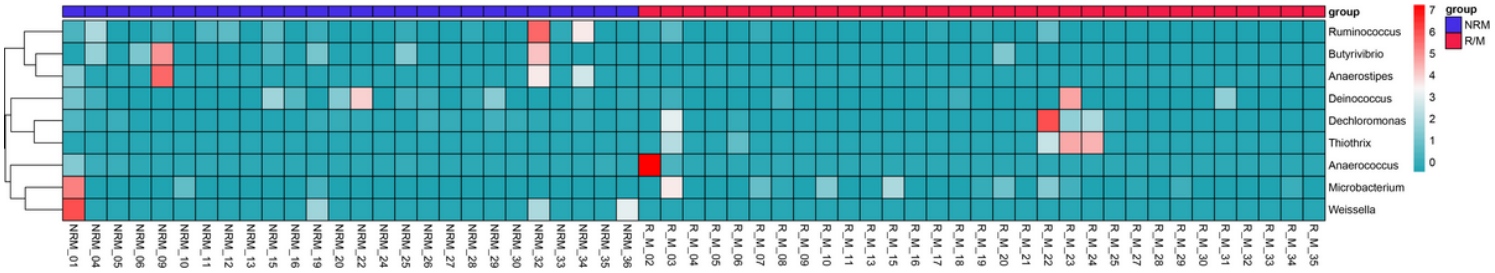

Figure 4

Heatmap of tumor microbiome differences at genus level between patients experiencing no recurrence or metastasis (NRM) and patients experiencing recurrence or metastasis (R/M).

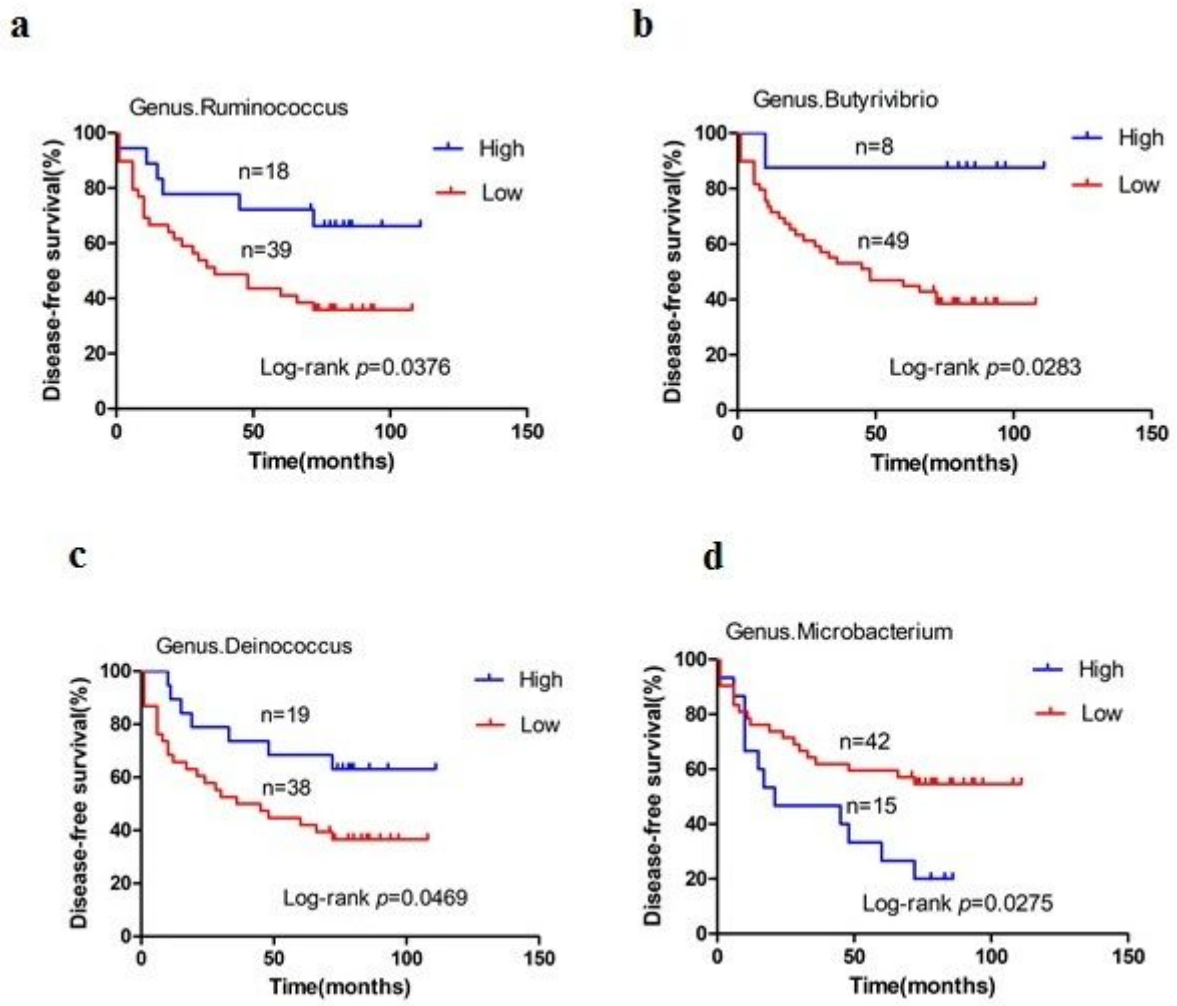

Figure 5

Kaplan-Meier estimates for disease-free survival (DFS) based on the abundance levels of microbes. a-c Kaplan-Meier estimates for DFS based on the abundance levels of microbes enriched at genus level in patients experiencing no recurrence or metastasis (NRM). Ruminococcus (a), Butyrivibrio (b), and Deinococcus (c). d Kaplan-Meier estimates for DFS based on the abundance levels of microbes that were enriched (at the genus level) in patients who experienced recurrence or metastasis (R/M).

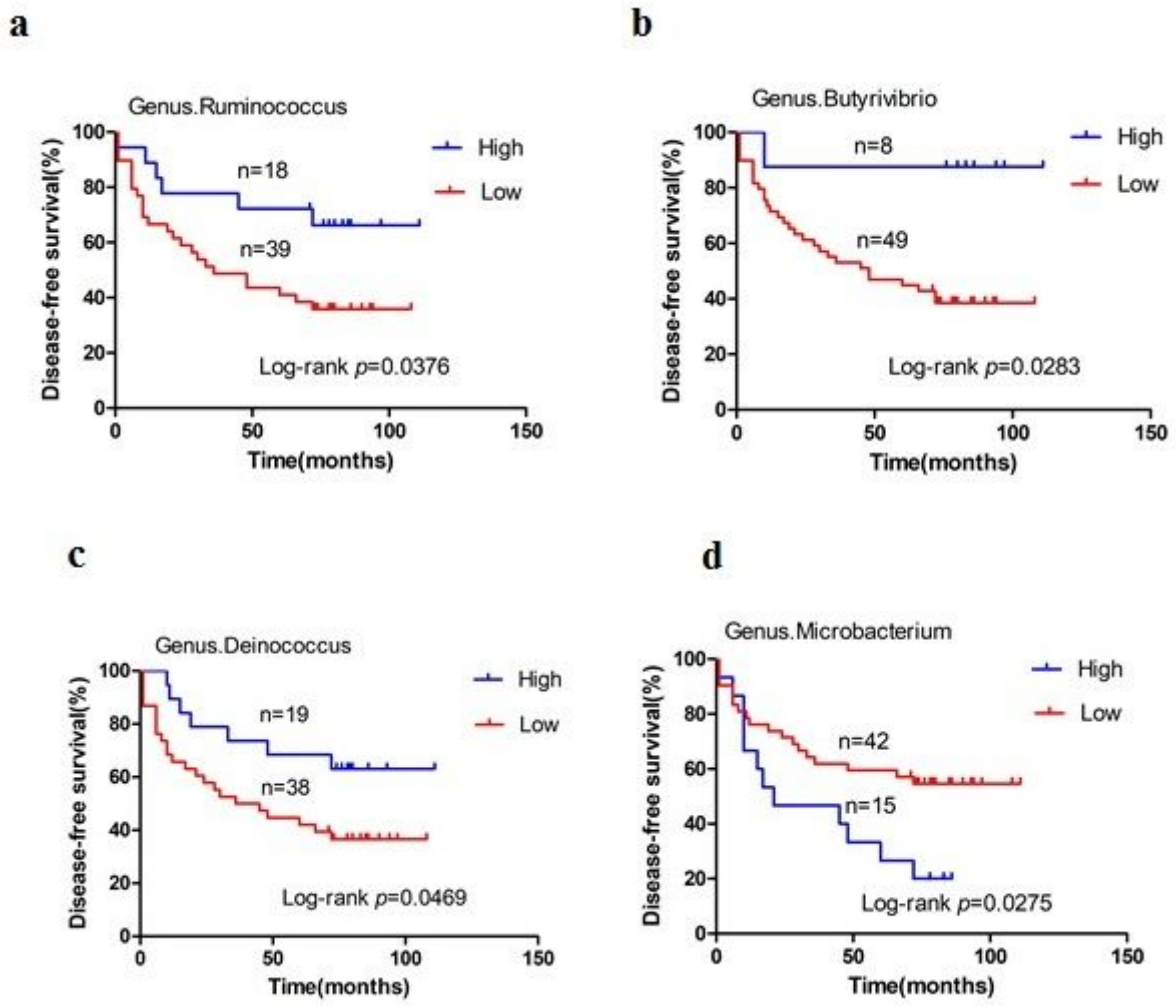

Figure 5

Kaplan-Meier estimates for disease-free survival (DFS) based on the abundance levels of microbes. a-c Kaplan-Meier estimates for DFS based on the abundance levels of microbes enriched at genus level in patients experiencing no recurrence or metastasis (NRM). Ruminococcus (a), Butyrivibrio (b), and Deinococcus (c). d Kaplan-Meier estimates for DFS based on the abundance levels of microbes that were enriched (at the genus level) in patients who experienced recurrence or metastasis (R/M).

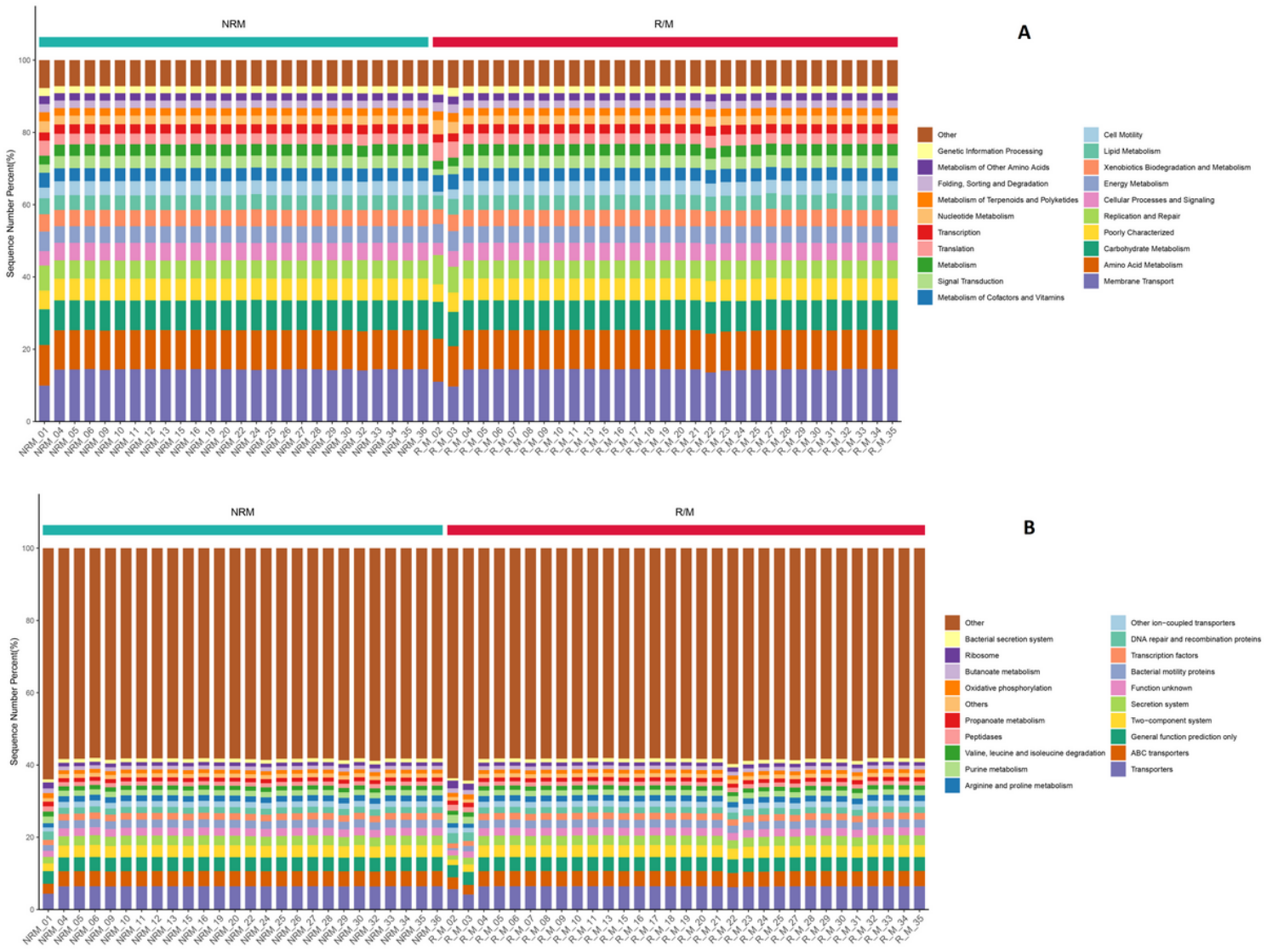

Figure 6

The top 20 predicted metagenomic functions at level 2 a and level 3 b of the Kyoto Encyclopedia of Genes and Genomes (KEGG) pathways.

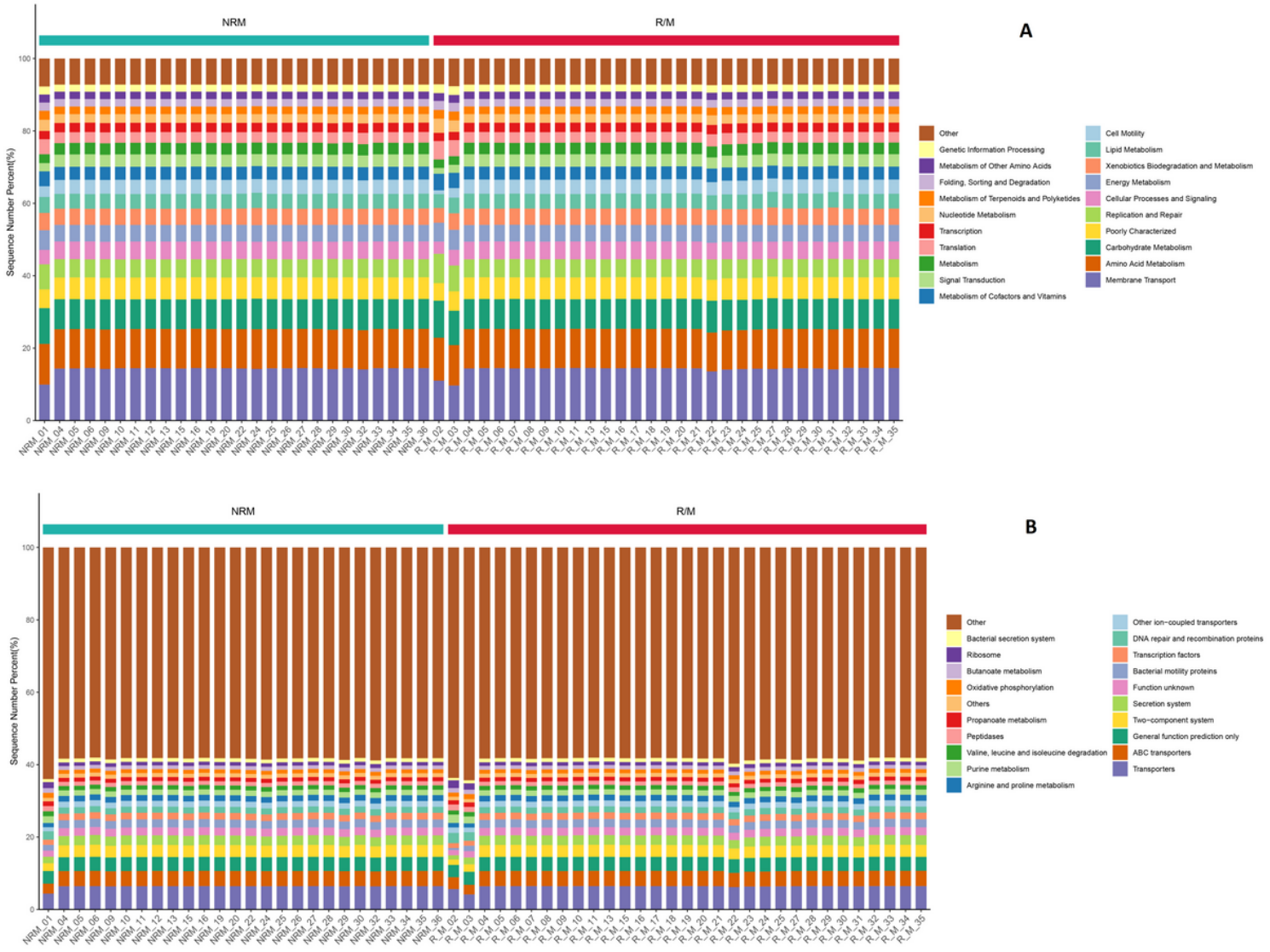

Figure 6

The top 20 predicted metagenomic functions at level 2 a and level 3 b of the Kyoto Encyclopedia of Genes and Genomes (KEGG) pathways.

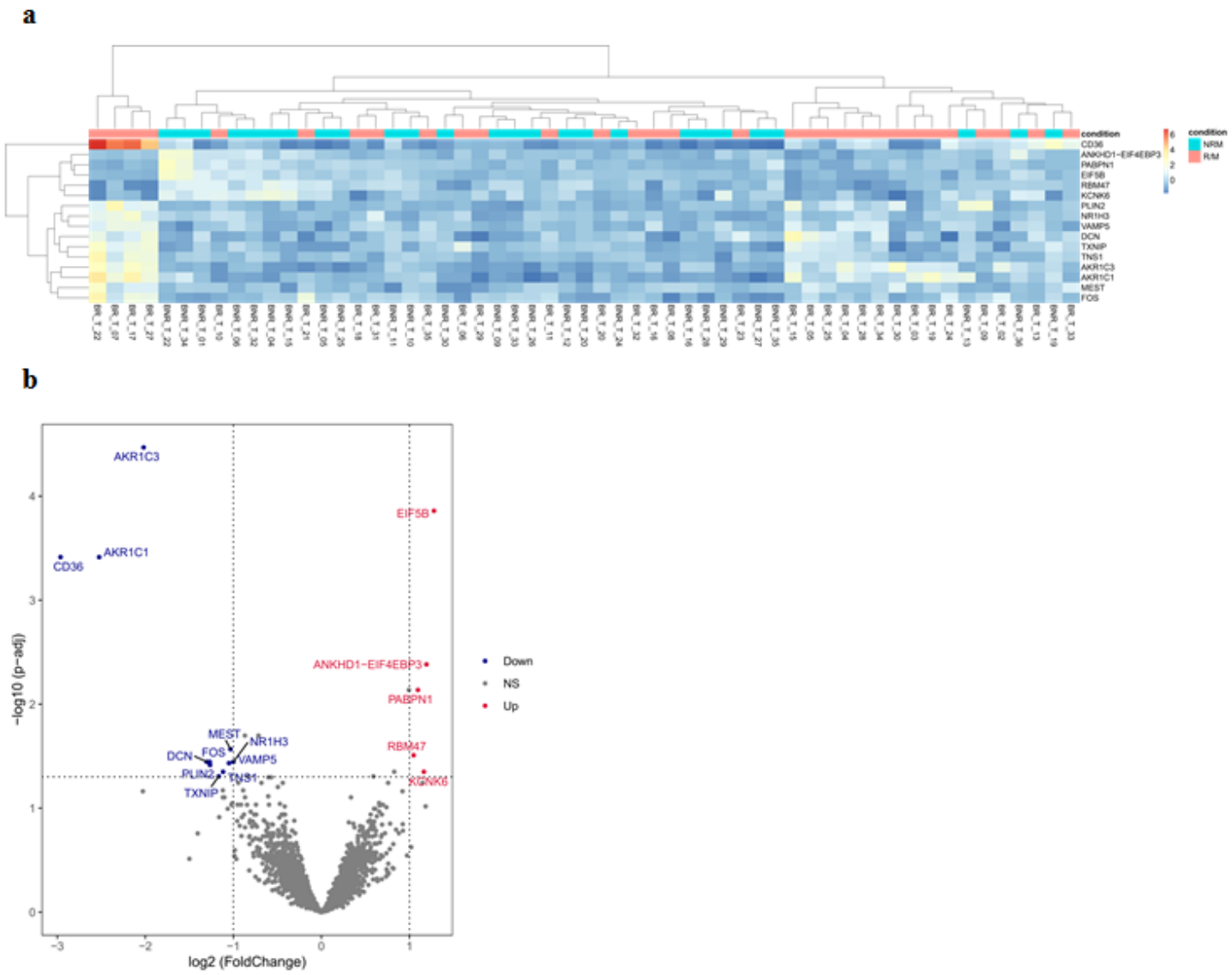

Figure 7

Differentially expressed genes (DEGs) between the two groups. a Heatmap of DEGs between the two groups. b Volcano plot for DEGs between the two groups. Red colour indicates up-regulated genes in patients experiencing no recurrence or metastasis; blue colour indicates down-regulated genes in those patients.

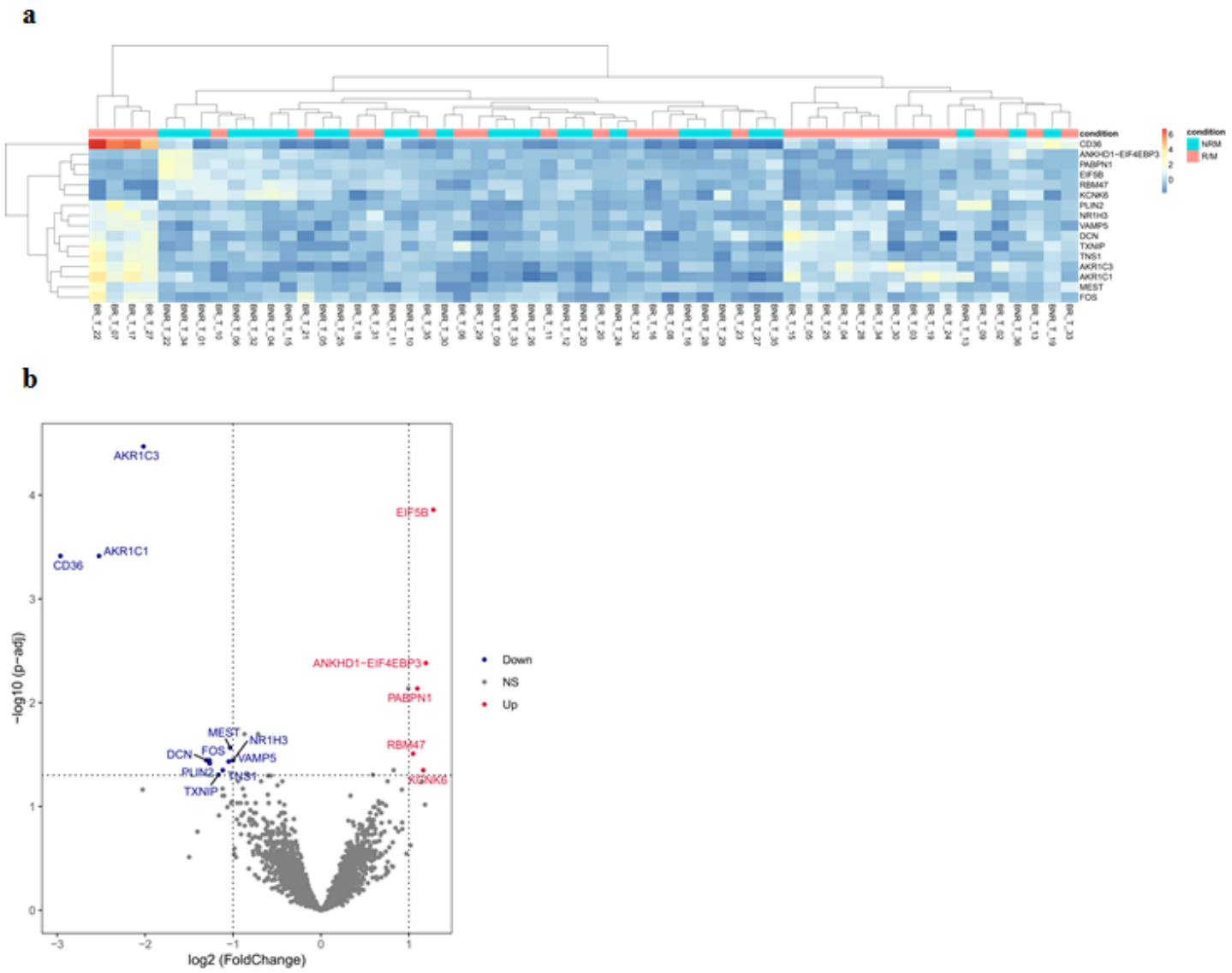

Figure 7

Differentially expressed genes (DEGs) between the two groups. a Heatmap of DEGs between the two groups. b Volcano plot for DEGs between the two groups. Red colour indicates up-regulated genes in patients experiencing no recurrence or metastasis; blue colour indicates down-regulated genes in those patients.

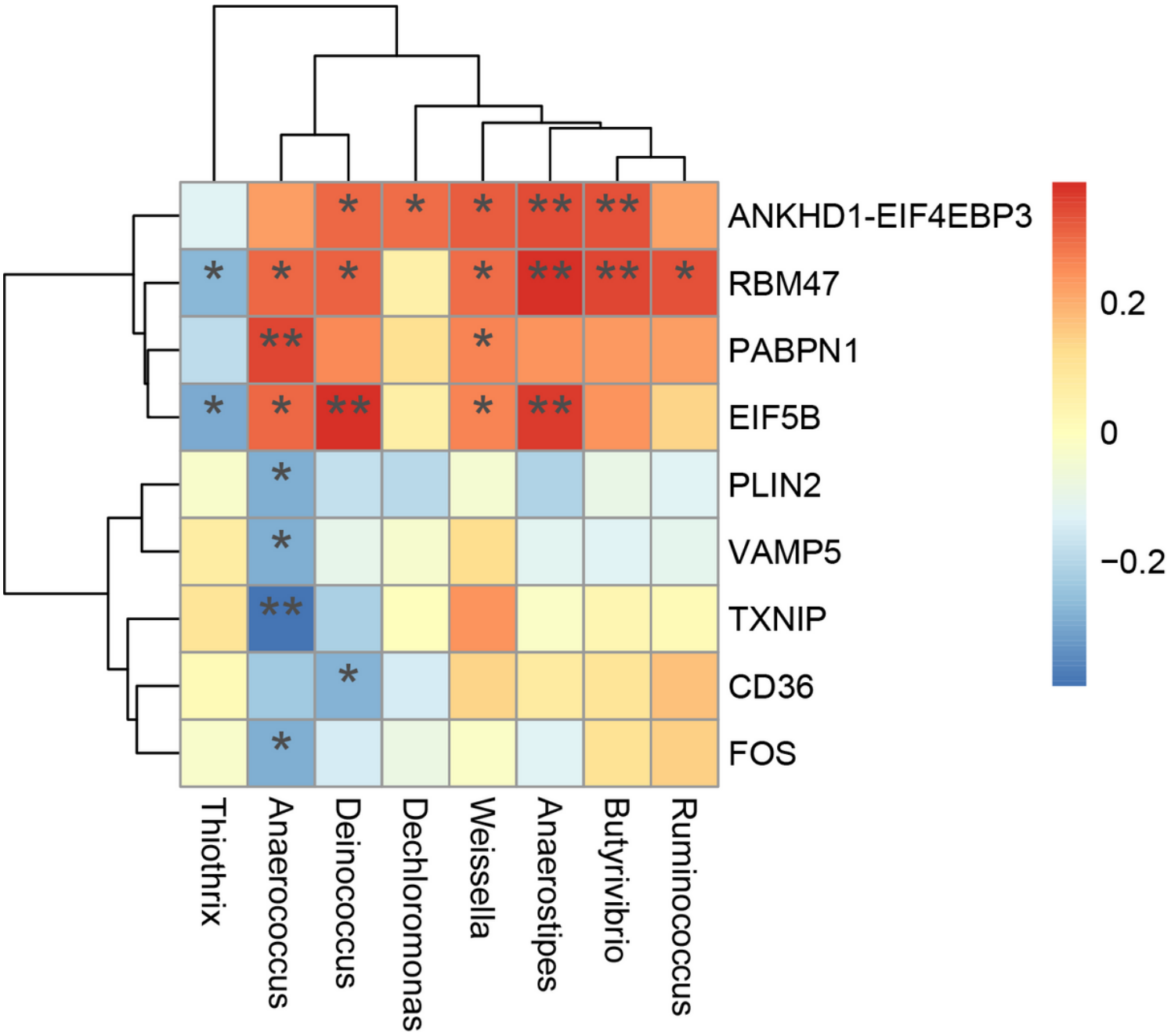

Figure 8

Associations between tumor microbiome differences and differentially expressed genes. *P < 0.05, **P < 0.01.

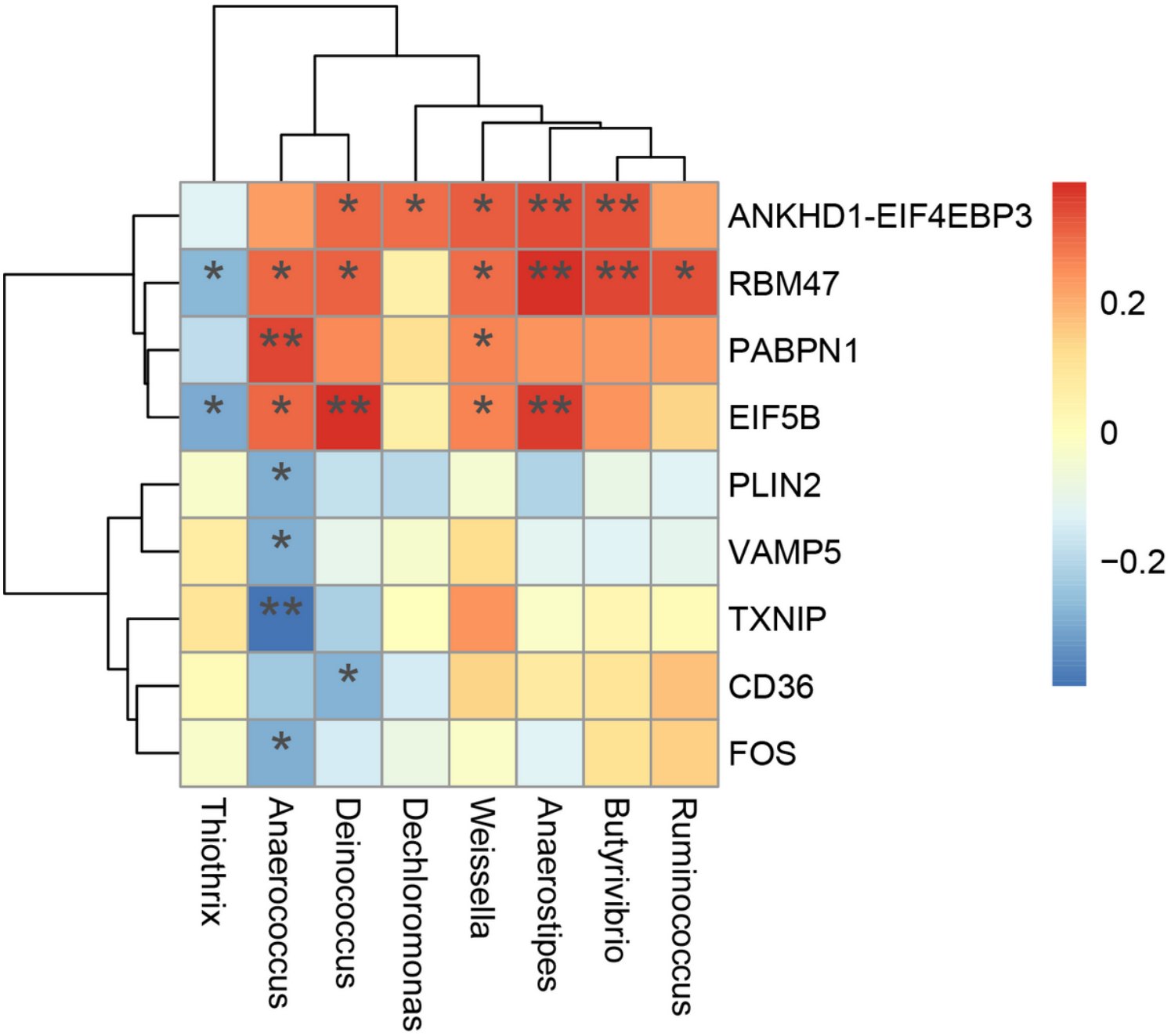

Figure 8

Associations between tumor microbiome differences and differentially expressed genes. *P < 0.05, **P < 0.01.

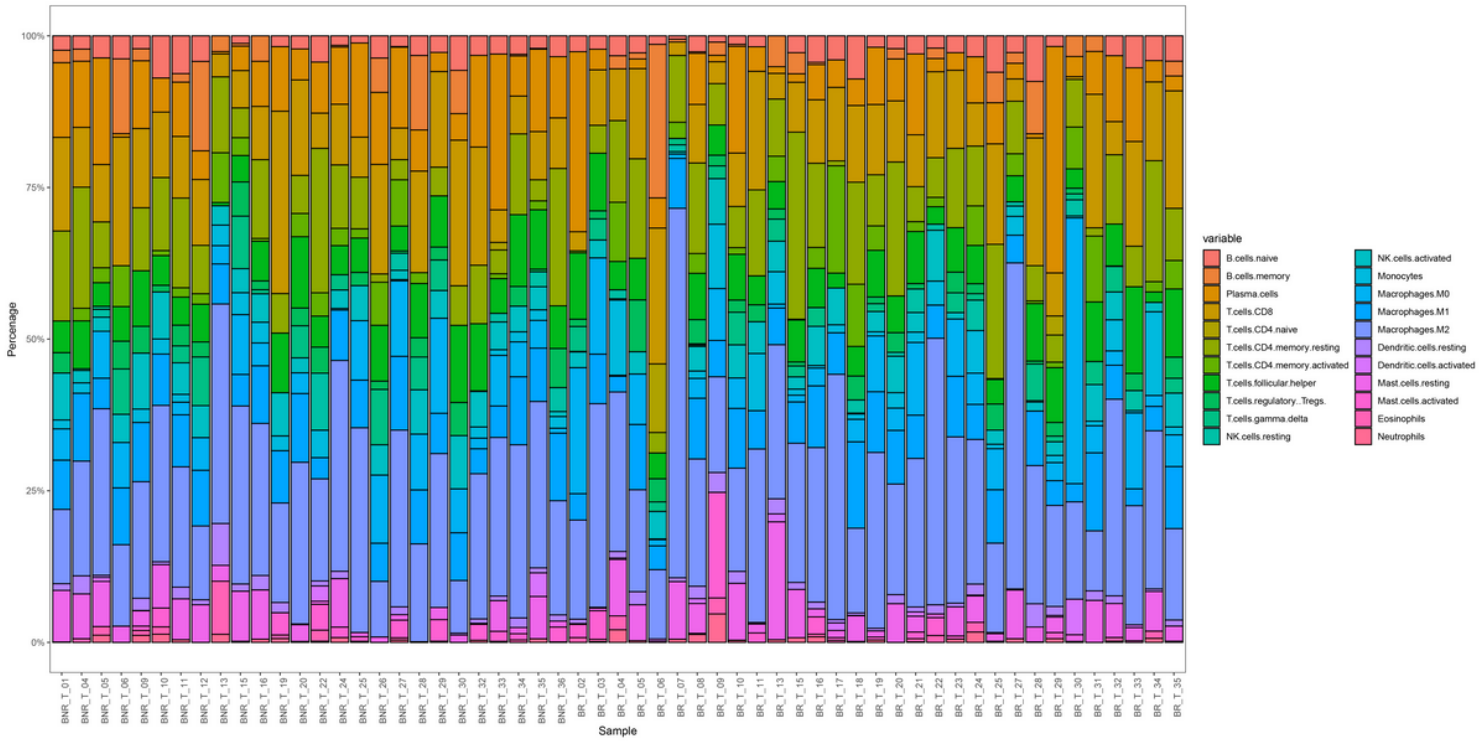

Figure 9

Relative proportions of the 22 tumor-infiltrating immune cell subpopulations in all tumor samples.

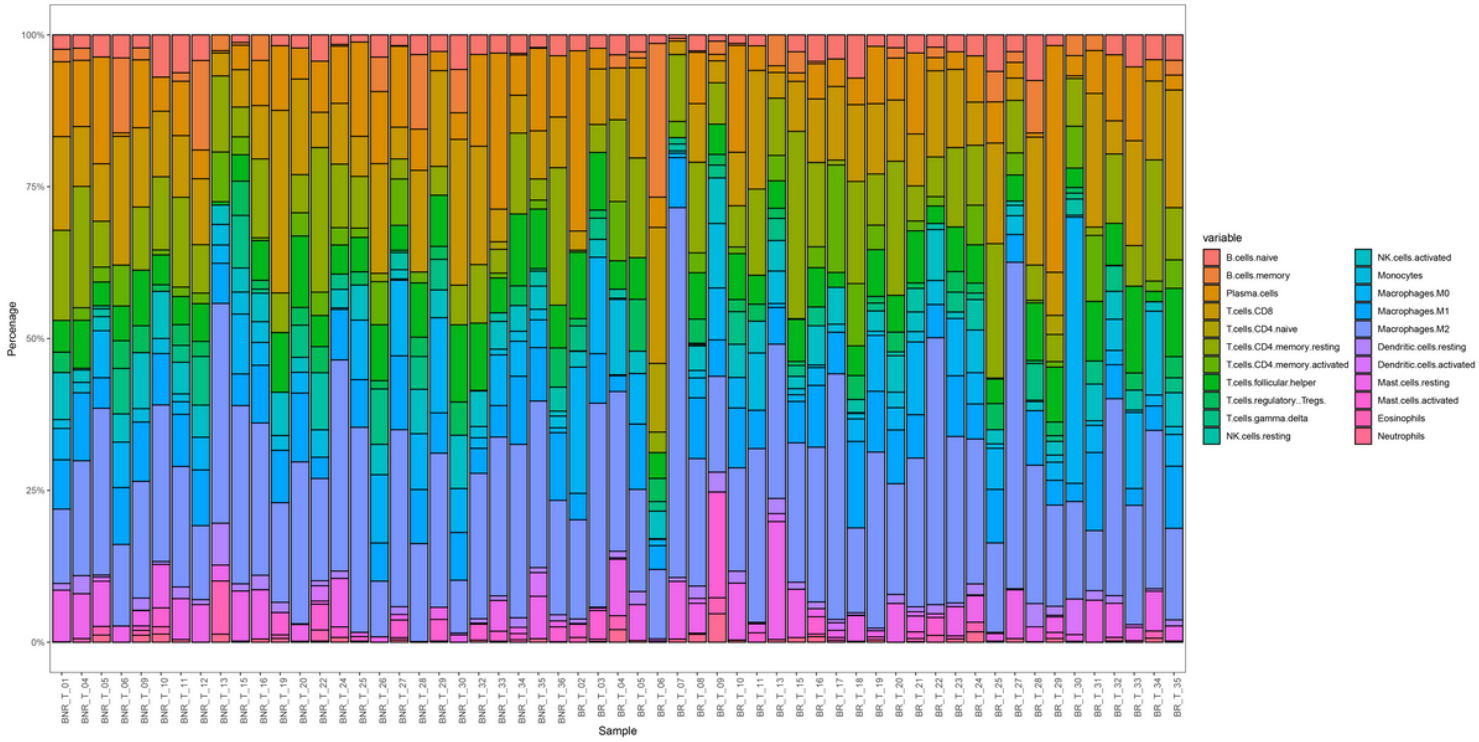

Figure 9

Relative proportions of the 22 tumor-infiltrating immune cell subpopulations in all tumor samples.

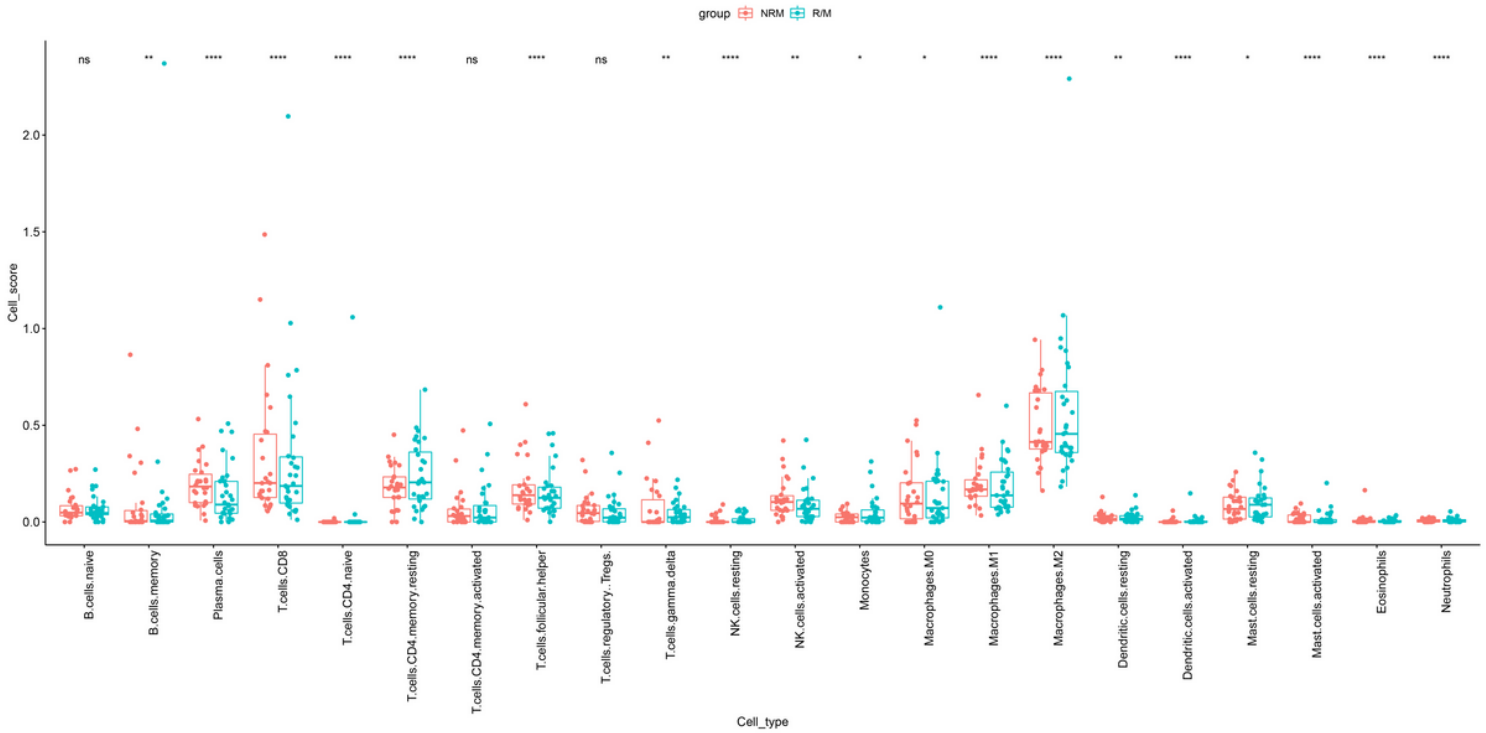

Figure 10

Boxplot presenting the differences in the 22 tumor-infiltrating immune cell subpopulations between patients experiencing no recurrence or metastasis (NRM) and patients experiencing recurrence or metastasis (R/M). *P<0.05, **P <0.01, ***P<0.001, ****P<0.0001.

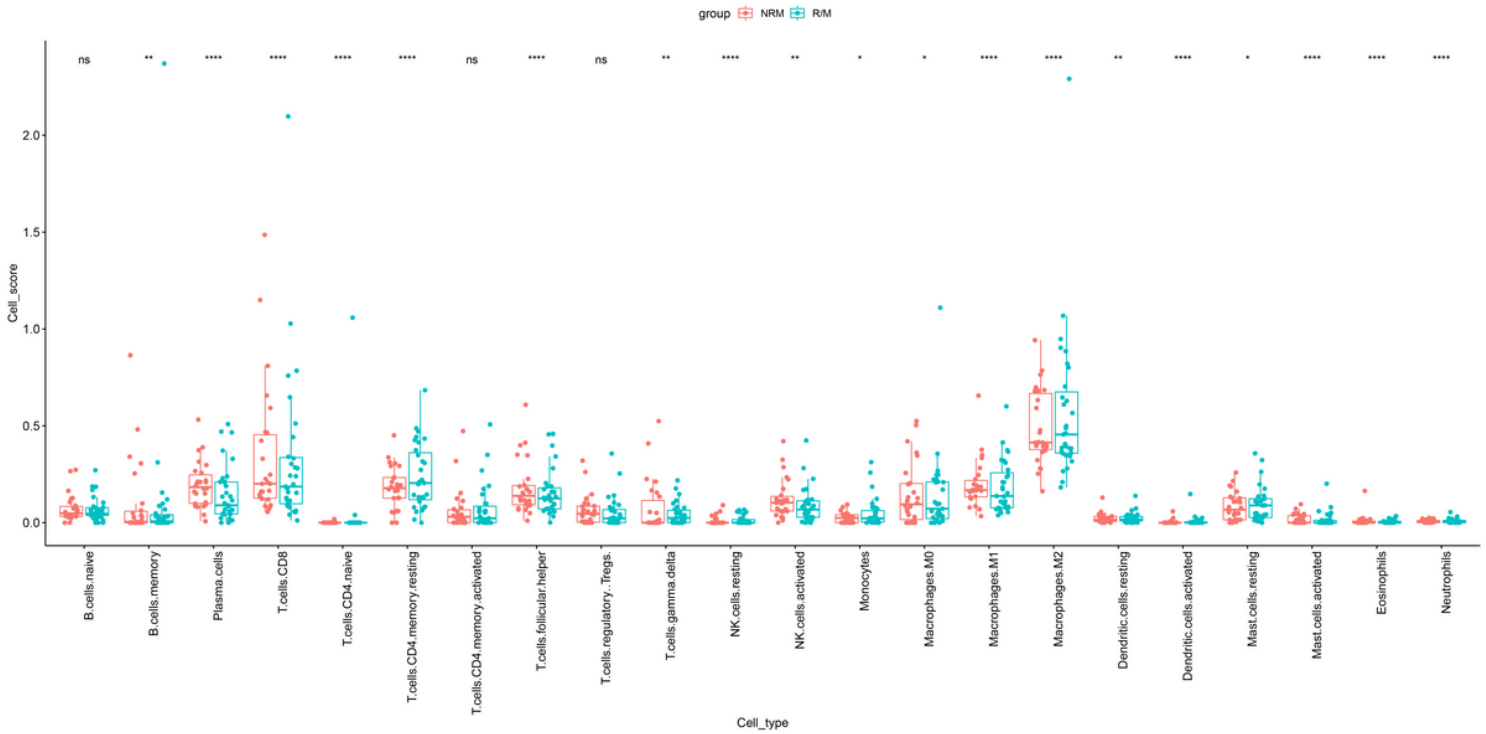

Figure 10

Boxplot presenting the differences in the 22 tumor-infiltrating immune cell subpopulations between patients experiencing no recurrence or metastasis (NRM) and patients experiencing recurrence or metastasis (R/M). *P<0.05, **P <0.01, ***P<0.001, ****P<0.0001.

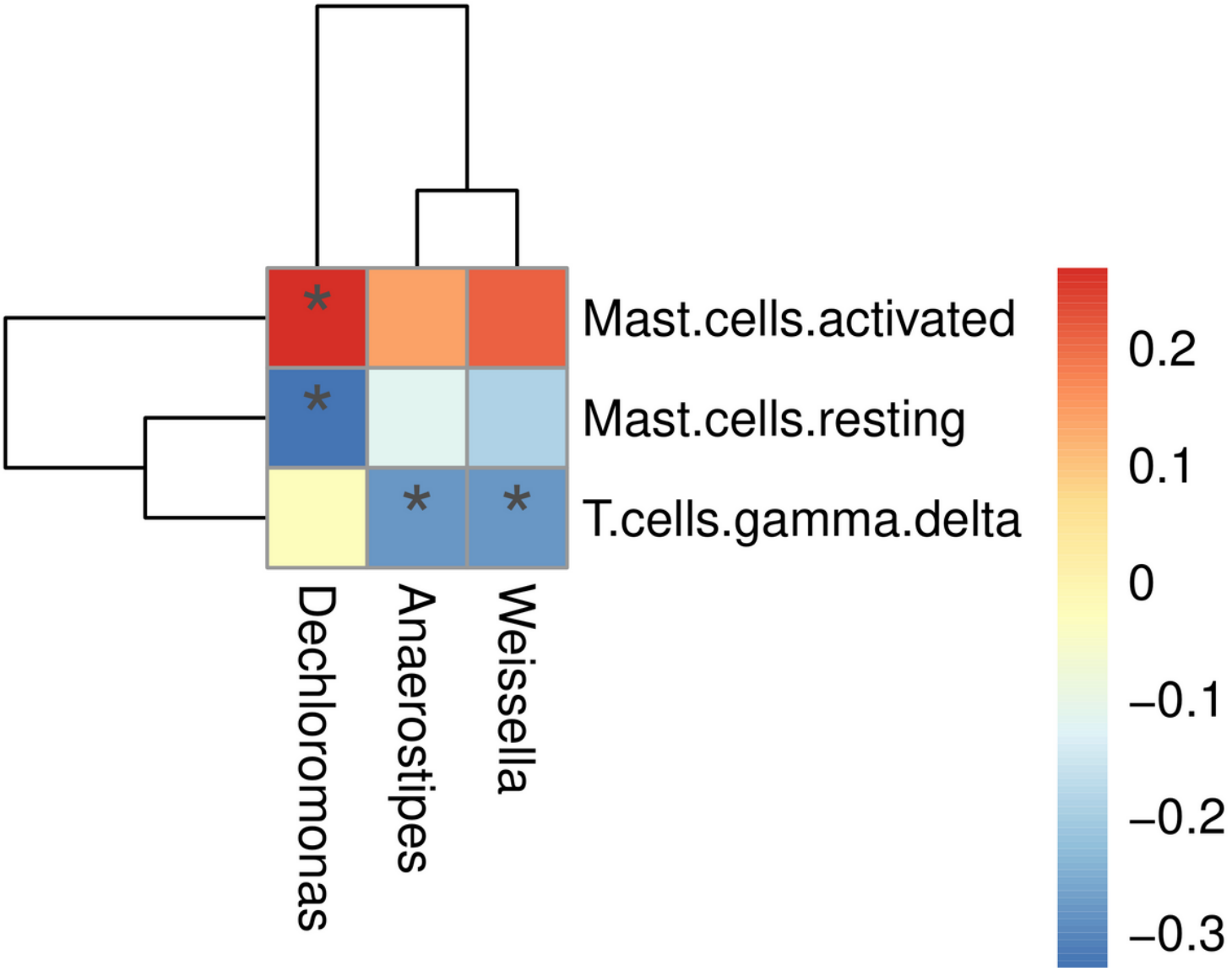

Figure 11

Associations between tumor microbiome differences and differences in tumor-infiltrating immune cell abundance. *P< 0.05.

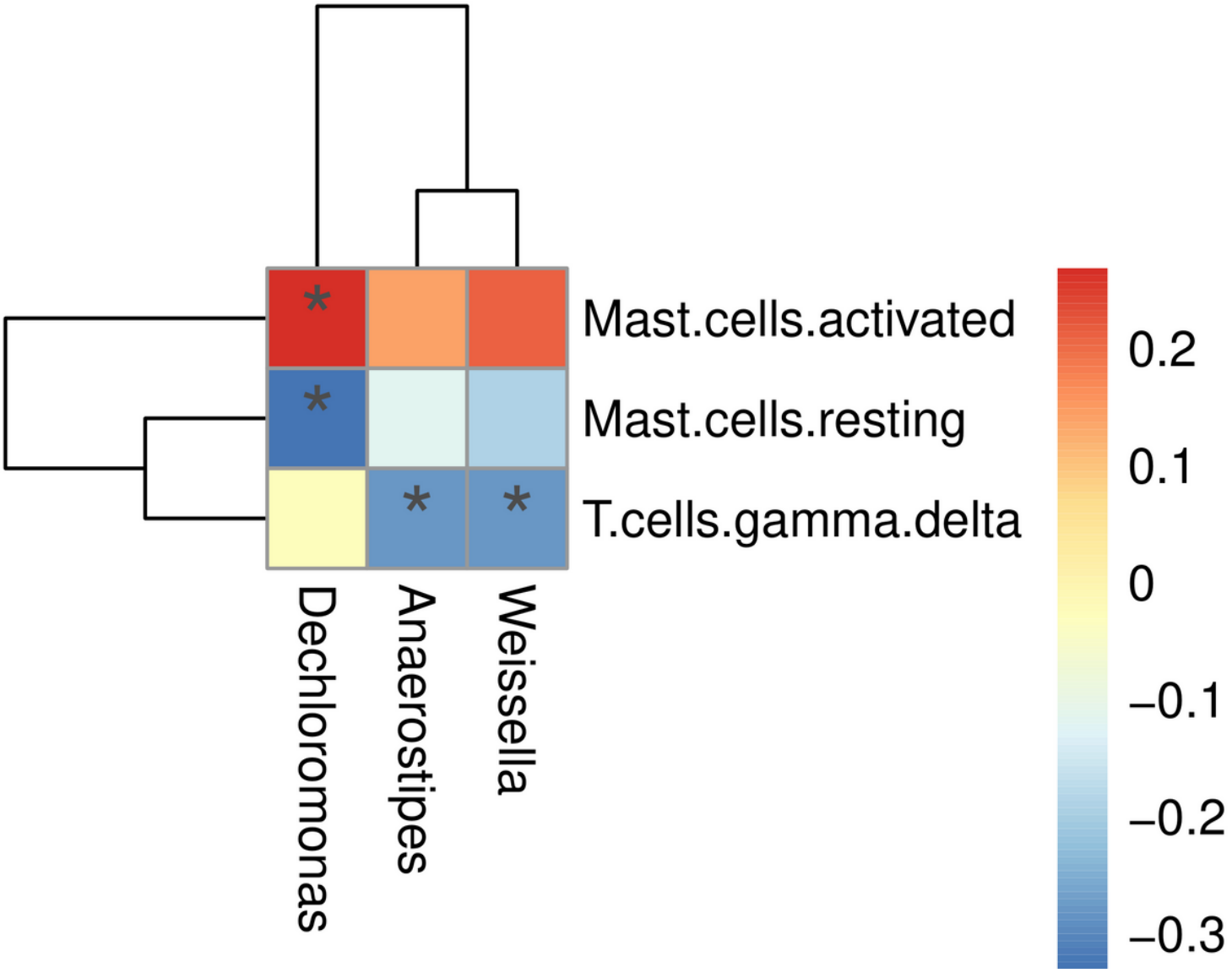

Figure 11

Associations between tumor microbiome differences and differences in tumor-infiltrating immune cell abundance. *P< 0.05.

Supplementary Files

This is a list of supplementary files associated with this preprint. Click to download.

- Additionalfile2.docx
- Additionalfile2.docx
- Additionalfile1.xlsx
- Additionalfile1.xlsx